EMPIRICAL ANALYSIS OF SMART ELECTRIC VEHICLE DRIVE SYSTEM

Project Supervisor: Engr. Tehseen Ilahi

Submitted By

Muhammad Rohail Akhtar

15029

Muhammad Umar Yaqoob

19201

Shukraan Mubarik

15427

Department of Electrical Engineering

Riphah International University, Pakistan

Certification

This is to certify that **Muhammad Rohail Akhtar 15029**, **Muhammad Umar Yaqoob 19201** and **Shukraan Mubarik 15427** have successfully completed the final project **Empirical Analysis of Smart Electric Vehicle Drive System** at the **Riphah International University** to fulfill the partial requirement of the **Electrical Engineering** degree.

External Examiner **Project Supervisor**

Chairman

Department of *Electrical Engineering*, Riphah International University

Empirical Analysis of Smart Electric Vehicle Drive System

Sustainable Development Goals

(Please tick the relevant SDG(s) linked with FYDP)

SDG No	Description of SDG	SDG No	Description of SDG
SDG 1	No Poverty	SDG 9 ☑	Industry, Innovation, and Infrastructure
SDG 2	Zero Hunger	SDG 10	Reduced Inequalities
SDG 3	Good Health and Well Being	SDG 11☑	Sustainable Cities and Communities
SDG 4	Quality Education	SDG 12 ☑	Responsible Consumption and Production
SDG 5	Gender Equality	SDG 13 ☑	Climate Change
SDG 6	Clean Water and Sanitation	SDG 14	Life Below Water
SDG 7 ☑	Affordable and Clean Energy	SDG 15	Life on Land
SDG 8 ☑	Decent Work and Economic Growth	SDG 16	Peace, Justice and Strong Institutions
		SDG 17	Partnerships for the Goals

Range of Complex Problem Solving			
	Attribute	**Complex Problem**	
1	Range of conflicting requirements	Involve wide-ranging or conflicting technical, engineering and other issues.	☑
2	Depth of analysis required	Have no obvious solution and require abstract thinking, originality in analysis to formulate suitable models.	☑
3	Depth of knowledge required	Requires research-based knowledge much of which is at, or informed by, the forefront of the professional discipline and which allows a fundamentals-based, first principles analytical approach.	☑
4	Familiarity of issues	Involve infrequently encountered issues	☑
5	Extent of applicable codes	Are outside problems encompassed by standards and codes of practice for professional engineering.	
6	Extent of stakeholder involvement and level of conflicting requirements	Involve diverse groups of stakeholders with widely varying needs.	
7	Consequences	Have significant consequences in a range of contexts.	☑
8	Interdependence	Are high level problems including many component parts or sub-problems	☑
Range of Complex Problem Activities			
	Attribute	**Complex Activities**	
1	Range of resources	Involve the use of diverse resources (and for this purpose, resources include people, money, equipment, materials, information and technologies).	☑
2	Level of interaction	Require resolution of significant problems arising from interactions between wide ranging and conflicting technical, engineering or other issues.	☑
3	Innovation	Involve creative use of engineering principles and research-based knowledge in novel ways.	☑
4	Consequences to society and the environment	Have significant consequences in a range of contexts, characterized by difficulty of prediction and mitigation.	☑
5	Familiarity	Can extend beyond previous experiences by applying principles-based approaches.	☑

Abstract

Designing vehicles based on sustainable energy sources is one of the topics of interest in all over the world now a day. The key is to accelerate the world's transition to sustainable energy. This project focuses on developing an efficient drive system for an electric car that could run on batteries. The project depicts the analysis, designing and simulation of an efficient drive system for three phase induction motor. The power handling capability of the system being developed is kept small scale for test purposes and can be scaled up after successful attempt.

In a nutshell, the project is based on designing of variable frequency drive (VFD) for the drive system which would control the speed mechanism of induction motor by changing frequency. A methodology is proposed to design EV drive system with control algorithm called Sinusoidal Pulse Width Modulation (SPWM). SPWM signal will switch the MOSFETs in such a way that a modified sine wave is produced at inverter output.

The modelling and simulation are developed in Proteus and with successful attempt locally available components are chosen for hardware implementation. IoT module and HMI interface is also incorporated with hardware system for better and efficient sensor communication and user-friendly interface. At the end data is collected and discussed in discussion section.

Keywords: EV; Electric Vehicle; Inverter; VFD; SPWM;

Undertaking

I certify that the project **Empirical Analysis of Smart Electric Vehicle Drive System** is our own work. The work has not, in whole or in part, been presented elsewhere for assessment. Where material has been used from other sources it has been properly acknowledged/ referred.

Muhammad Rohail Akhtar

15029

Muhammad Umar Yaqoob

19201

Shukraan Mubarik

15427

Acknowledgement

This thesis has been a transformative journey for us, and we are deeply grateful to all those who have contributed to its realization.

First and foremost, we express our heartfelt gratitude to our esteemed supervisor Engineer Tehseen Ilahi. Your guidance, expertise, and unwavering support have been instrumental in shaping this research. Your patience, encouragement, and insightful feedback have motivated us to strive for excellence in every aspect of this work.

We extend our sincere thanks to the faculty and staff of Riphah International University, Department of Electrical Engineering, whose dedication to fostering a vibrant academic environment has enriched our learning experience. The stimulating discussions, seminars, and resources provided have been invaluable in shaping the trajectory of this project.

We would like to acknowledge the participants of the evaluation board, whose valuable contributions and willingness to engage in the assessment process have made this work possible. Their perspectives have shed light on critical aspects of the subject matter and have enriched the quality of this work.

Lastly, we offer our deepest gratitude to ALLAH Almighty for guiding us through this academic pursuit, providing us with the resilience to overcome challenges, and blessing us with the wisdom to pursue knowledge.

Each person and entity mentioned here has played a significant role in the completion of this project. Their collective influence has left an indelible mark on my academic and personal growth. This accomplishment would not have been possible without their unwavering support, encouragement, and belief in our abilities.

Thank you all for being a part of this remarkable journey, and for helping us turn this project into a reality.

TABLE OF CONTENTS

List of Figures

List of Tables

List of Acronyms

AC	Alternating Current
AWS	Amazon Web Services
BJT	Bipolar Junction Transistor
BOM	Bill of Materials
CO_2	Carbon Dioxide
DC	Direct Current
EEPROM	Electrically Erasable Programmable Read-Only Memory
EV	Electric Vehicle
FET	Field Effect Transistor
GUI	Graphical User Interface
HMI	Human-Machine Interface
I/O	Input/Output
I2C	Inter-Integrated Circuit
IDE	Integrated Development Environment
IGBT	Insulated Gate Bipolar Transistor
IoT	Internet of Things
KB	Kilo Bytes
LCD	Liquid Crystal Display
MOS	Metal Oxide Semiconductor
MOSFET	Metal Oxide Semiconductor Field Effect Transistor
PWM	Pulse Width Modulation
SPI	Serial Peripheral Interface
SPWM	Sinusoidal Pulse Width Modulation
SRAM	Static Random-Access Memory
SVPWM	Space Vector Pulse Width Modulation
TFT	Thin-Film Transistor
TWI	Two-Wire Interface

UART	Universal Asynchronous Receiver / Transmitter
USART	Universal Synchronous/Asynchronous Receiver/Transmitter
USB	Universal Serial Bus
V/f	Voltage/Frequency
VFD	Variable Frequency Drive

Chapter 1

1 INTRODUCTION

1.1 Project Introduction

In today's world, the use of fossil fuels like coal, oil, and natural gas has led to significant environmental consequences. The combustion of these fuels for energy and transportation has resulted in widespread pollution, affecting ecosystems and human health. This has led to the release of substantial amounts of carbon dioxide (CO2) and other greenhouse gases into the atmosphere, contributing to a notable environmental challenge [1]. Additionally, it's crucial to recognize the finite nature of oil as a primary energy source, as it's being depleted on a global level [2].

However, there is a rising focus on exploring clean, renewable energy alternatives to mitigate these problems. To address the reliance on oil in transportation, adopting electric vehicles (EVs) emerges as a practical remedy. EVs have advanced significantly in various forms like cars, scooters, bicycles, and even electric wheelchairs [3].

This project aims to develop a functional electric drive system using an induction motor, powered by DC batteries. The key idea is to design a variable frequency drive (VFD) to control the drivetrain's speed. Induction motors paired with Variable Frequency Drives (VFDs) integrated into electric vehicles (EVs) with smart features optimize electric vehicle (EV) performance, delivering advanced performance and efficiency. Induction motors offer reliable propulsion, while VFDs ensure precise speed and torque control. This combination improves energy efficiency, regenerative braking, smooth acceleration, and adaptability to different driving conditions. The addition of smart features enhances connectivity, data analysis, and autonomous capabilities, driving EVs toward sustainable, intelligent, and enhanced driving experiences [4].

1.2 Block Diagram of EV Drive System

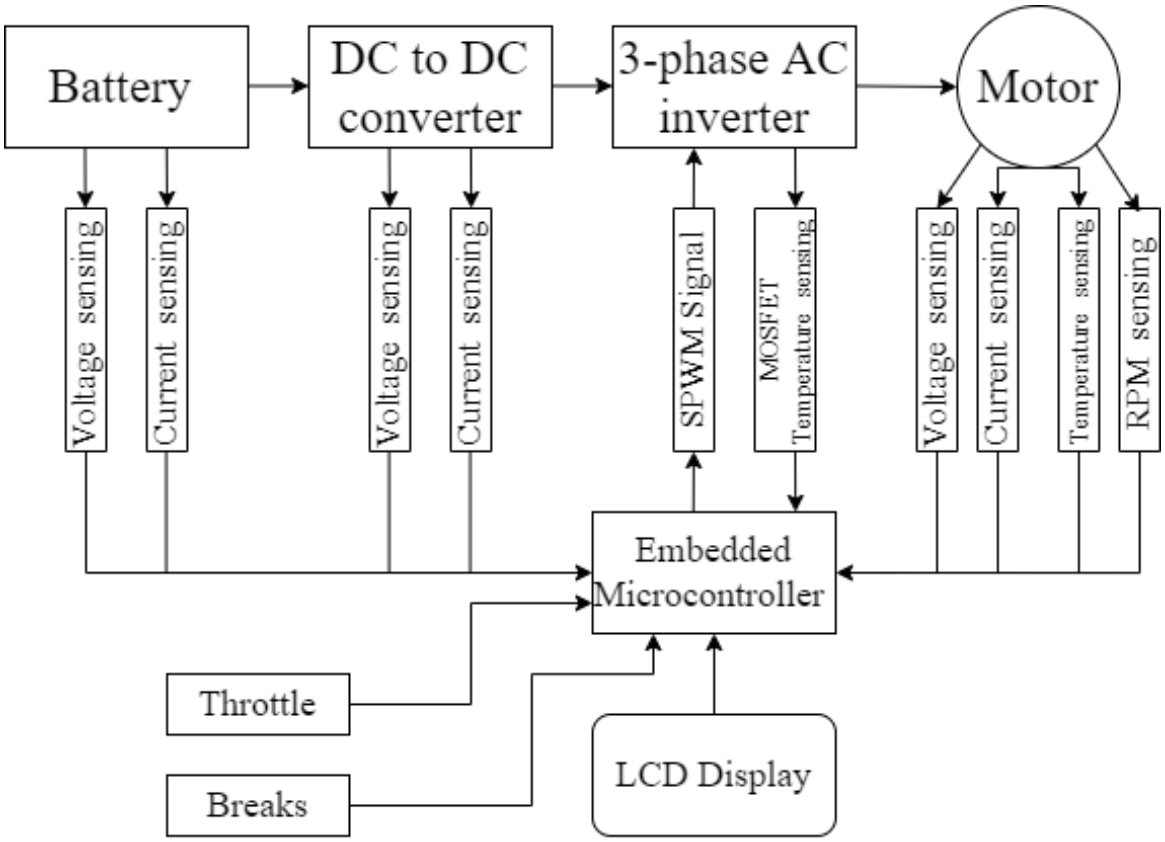

Figure 1-1: EV Drive System Block diagram

This Block Diagram illustrates the design scheme of EV Drive with major components such as Battery, DC to DC converter, 3-phase AC inverter, Electric Motor and Embedded Microcontroller [5]. Whereas voltage, current, and Temperature sensor are used as Feedback response. Furthermore, Embedded Microcontroller is used to control the operation of 3-phase AC inverter which control the speed of motor.

1.3 Approach

In the designing of this project the first step is to design a 24V, low voltage three phase induction motor, in order to operate at safe voltages. This is done to avoid the need for power electronics circuitry such as DC-DC Boost converter to raise the voltage level of batteries to the commonly available three phase induction motors which is rated at 400V. Then a high power three phase inverter has been designed to drive this induction motor. With the aid of Arduino MEGA microcontroller and the sinusoidal pulse width modulation (SPWM) technique, this inverter has been effectively controlled. Arduino MEGA has high power computational capability to accurately run the SPWM algorithm, while being in compact form factor.

Arduino MEGA serves another major purpose of regulating the speed and supply current to the induction motor. This is done by incorporating V/f control algorithm with SPWM algorithm. In V/f control as the ratio is kept constant by either changing supply voltage or supply frequency. Thus the speed motor is controlled.

1.4 3-phase inverter

A three-phase inverter is a fundamental electrical device that converts direct current (DC) into three-phase alternating current (AC). It's essential for various applications like industrial machines, renewable energy, and electric vehicles. This inverter takes DC power and generates three AC waveforms, each phase spaced 120 degrees apart. Different types of three-phase inverters exist, such as voltage-source inverters (VSI) and current-source inverters (CSI), each suited for specific uses.

1.4.1 Working of a 3-phase inverter

To simplify and easily explain the working of three phase inverter we will assume an ideal circuit with ideal switches. Given below is the circuit diagram idealized using six switches. As you can see this setup with six mechanical switches is more useful in understanding the 3-phase inverter working than using the actual transistor circuit.

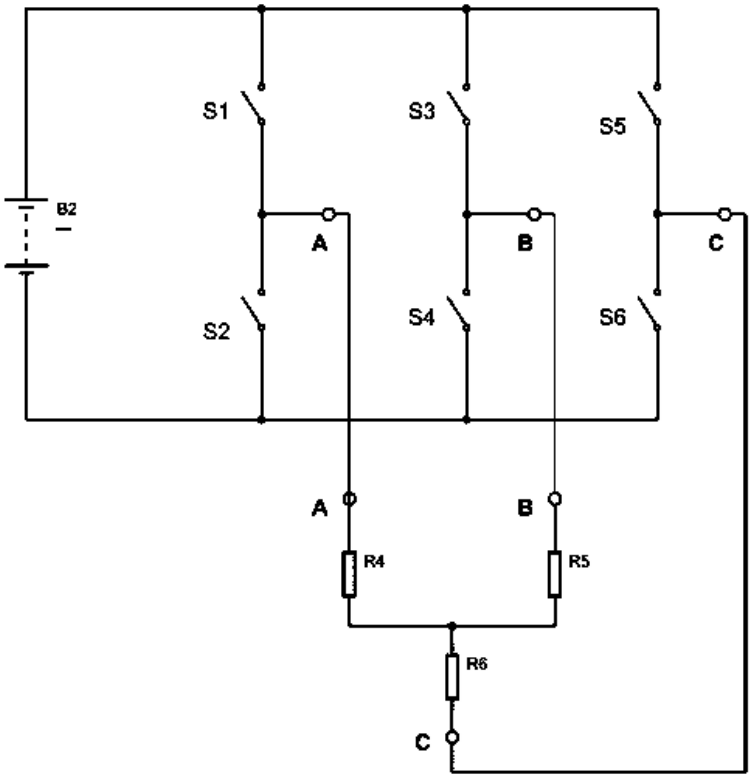

Figure 1-2: Operation of 3-phase inverter

1.4.2 180-Degree Conduction Mode

In the 180-degree conduction mode, each phase leg of the inverter operates for 180 degrees of the fundamental AC waveform. This means that each phase leg conducts for half of the AC cycle (from 0 to 180 degrees) and remains switched off for the other half. During conduction, the voltage across the load is positive, and during the off period, it's zero.

Let's see the working of a 3-phase inverter with the help of ideal switch circuit made earlier. The circuit is divided into three segments namely segment one, segment two & segment three. Segment one consists of a pair of switches S1&S2, segment two consists of switching pair S3&S4 and segment three consists of switching pair S5&S6. At any given time both the switches in the same segment should never be closed as it leads to battery short circuits failing the entire setup, so this scenario should be avoided at all times.

Now let's start switching sequence by closing the switch S1 in the first segment of the ideal circuit and let's name the start as 0º. Since the selected time of conduction is 180º the switch S1 will be closed from 0º to 180º. After 120º of the first segment, the second segment will also have a closed switch so, switch S3 will be closed. This S3 will also be kept closed for another 180º. Similarly, the third segment also has a switch closed after 120º so, switch S5 will be closed after 120º S3 closing i.e., 240º of switch S1. It is noteworthy that in the same segment both switches should never be in the closed position at the same time, so if one switch is closed then another must be open.

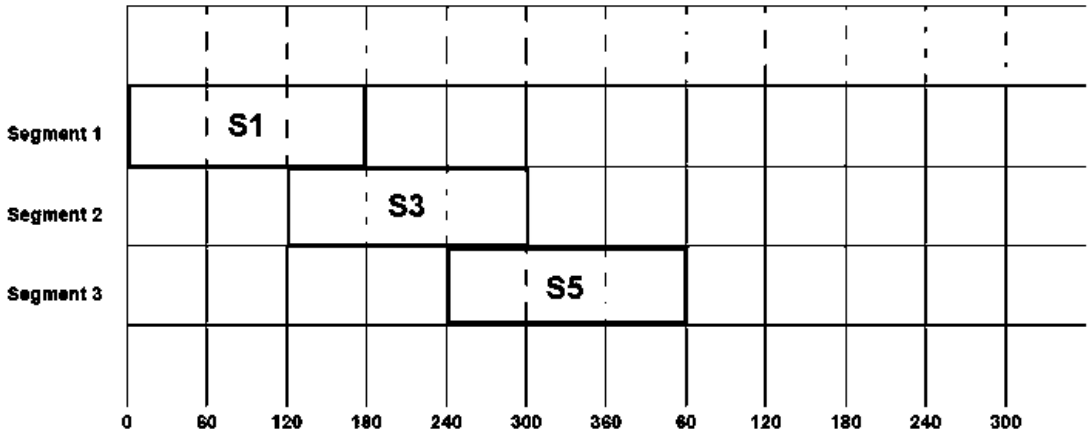

Figure 1-3: Switching sequence of upper switches

Now to complete the switching loop we will close S2, S4& S6 in a predetermined order. So only after S1 gets opened we will have to close S2. Similarly, S4 will be closed after S3 gets opened and in the same way S6 will be closed after S5 completes the conduction cycle.

This cycle of switching between switches of the same segment can be seen below figure. Here S2 followsS1, S4 follows S3 and S6 follows S5.

Figure 1-4: Complete switching sequence

The continuous wave forms after switching are given below.

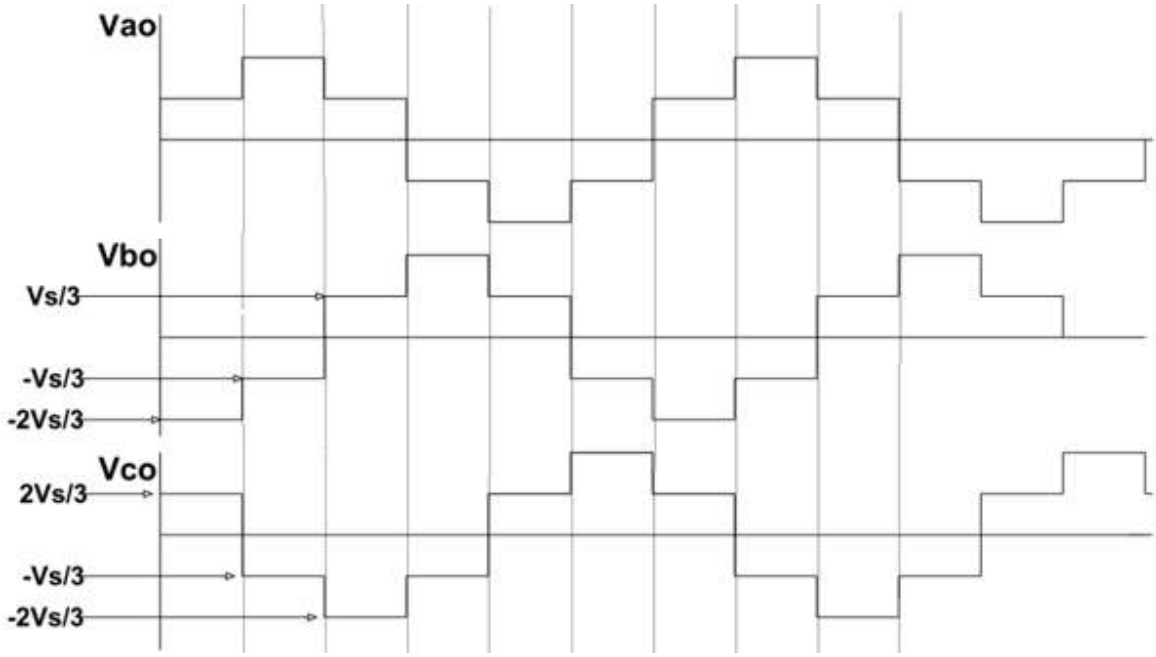

Figure 1-5: Phase to neutral voltage waveforms

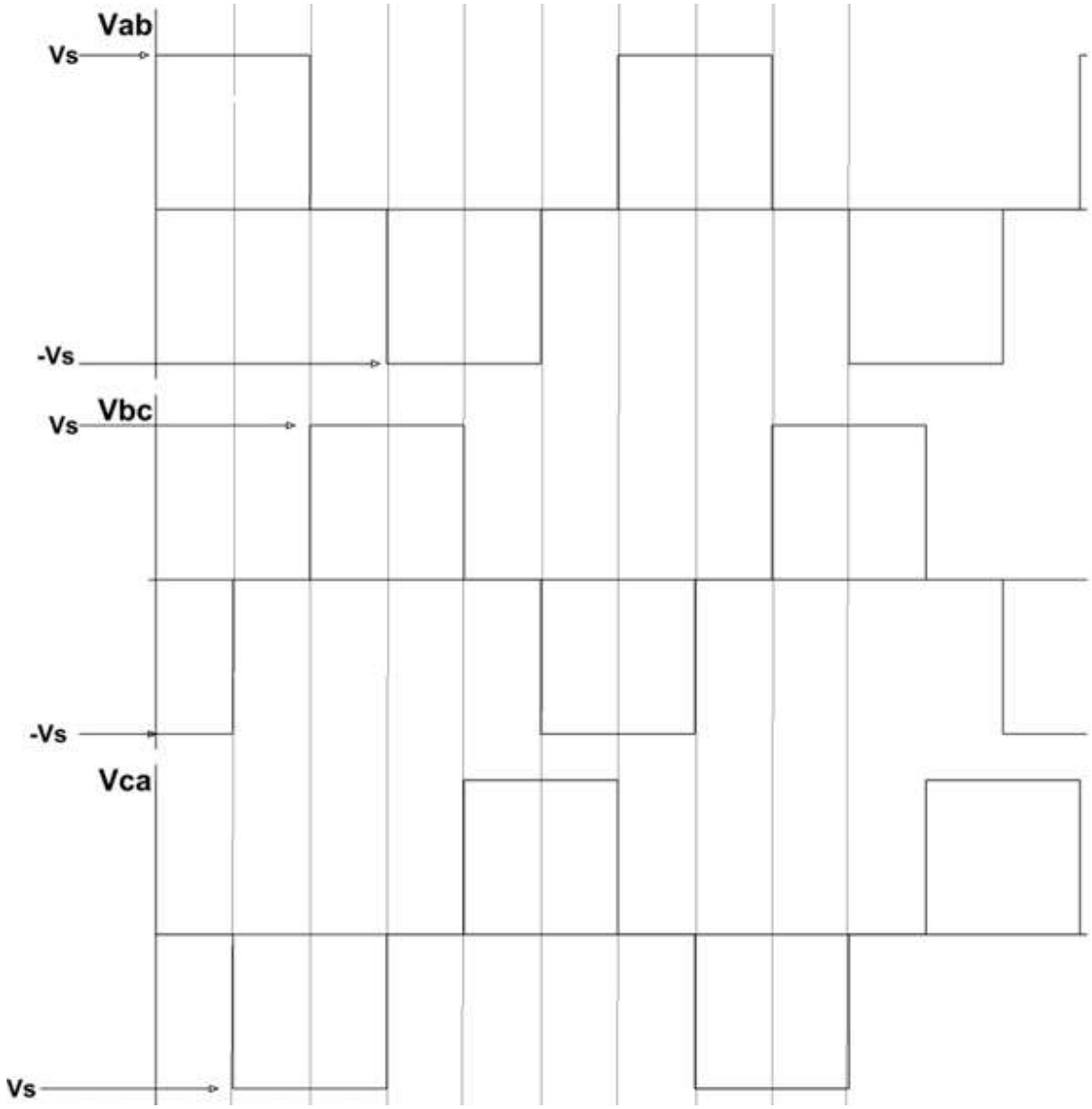

Figure 1-6: Phase to phase voltage waveforms

This mode has the advantage of reduced harmonic content in the output waveform, while only two out of the three phases are active at any given time, it results in a lower average output voltage compared to the 120-degree conduction mode and to achieve the same output voltage it requires a larger DC voltage source.

1.4.3 120-Degree Conduction Mode:

In the 120-degree conduction mode, each phase leg of the inverter operates for 120 degrees of the fundamental AC waveform. This mode results in a more continuous output waveform compared to the 180-degree mode. Each phase leg conducts for one-third of the AC cycle (from 0 to 120 degrees) and remains switched off for the remaining period. All three phases

are active during different parts of the cycle, allowing for a smoother output waveform with less voltage ripple.

As similar to the 180-degree conduction mode, the 120-degree conduction mode will also use the ideal switch circuit for its realization. Let's start switching sequence by closing the switch S1 in the first segment and be the start number to 0º. Since the selected time of conduction is 120º the switch S1 will be opened after 120º. Now after 120º of the first segment, the second segment switch S3 will be closed. This S3 will also be kept closed for another 120º. So S3 will be closed from 120º to 240º. Following is the third segment switch S5, which will be closed after 120º of S3 closing. Once the switch is closed, it will be kept closed for coming 120º before being opened and with that, the switch S5 will be closed from 240º to 360º.

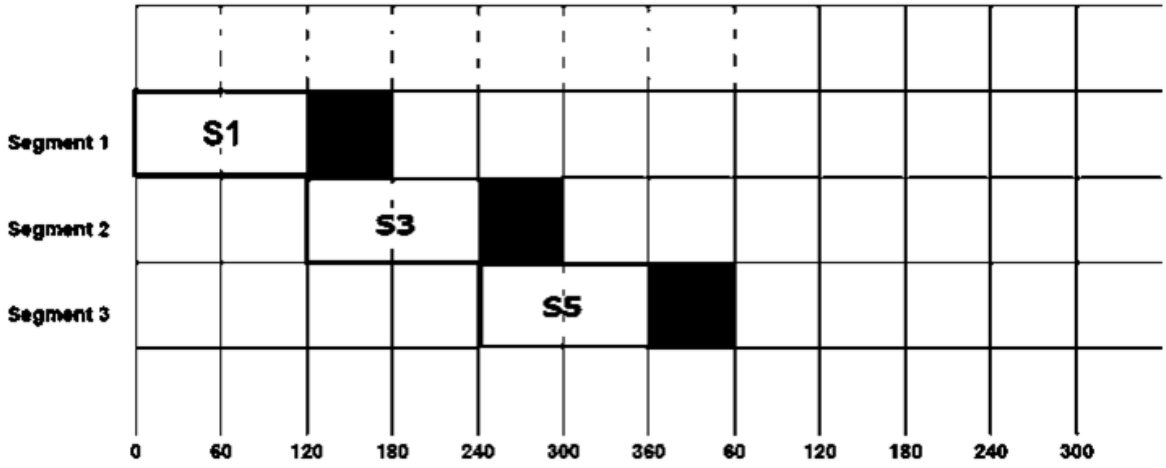

Figure 1-7: Switching sequence of upper switches

This cycle of symmetrical switching will be continued for achieving the desired three-phase voltage. If we fill in the beginning and ending switching sequence in the above table, we will have a complete switching pattern for 120º conduction mode as below.

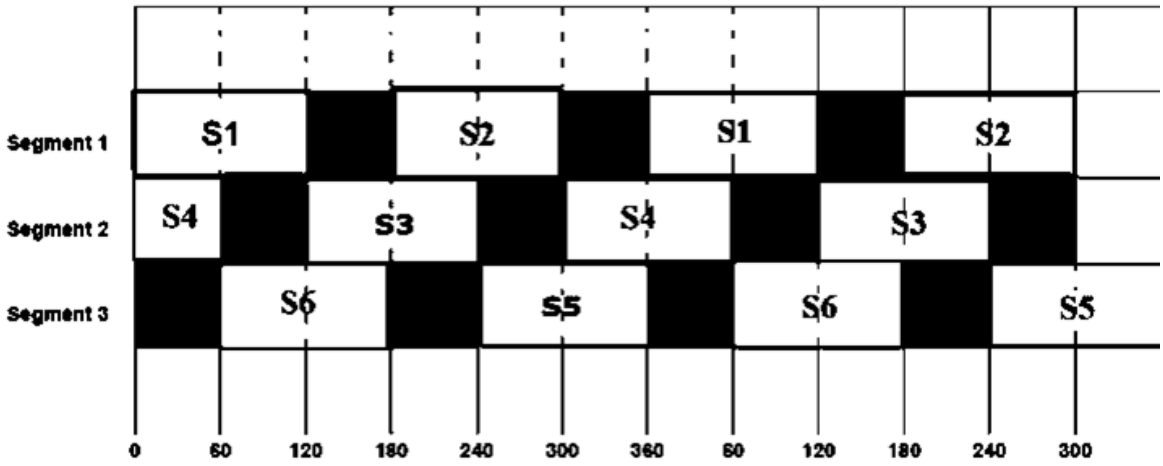

Figure 1-8: Complete switching sequence

However, this mode can introduce more harmonics into the output voltage compared to the 180-degree conduction mode. Similar to the 180-degree mode, this is not usually considered a modulation technique on its own.

The continuous wave forms after switching are given below.

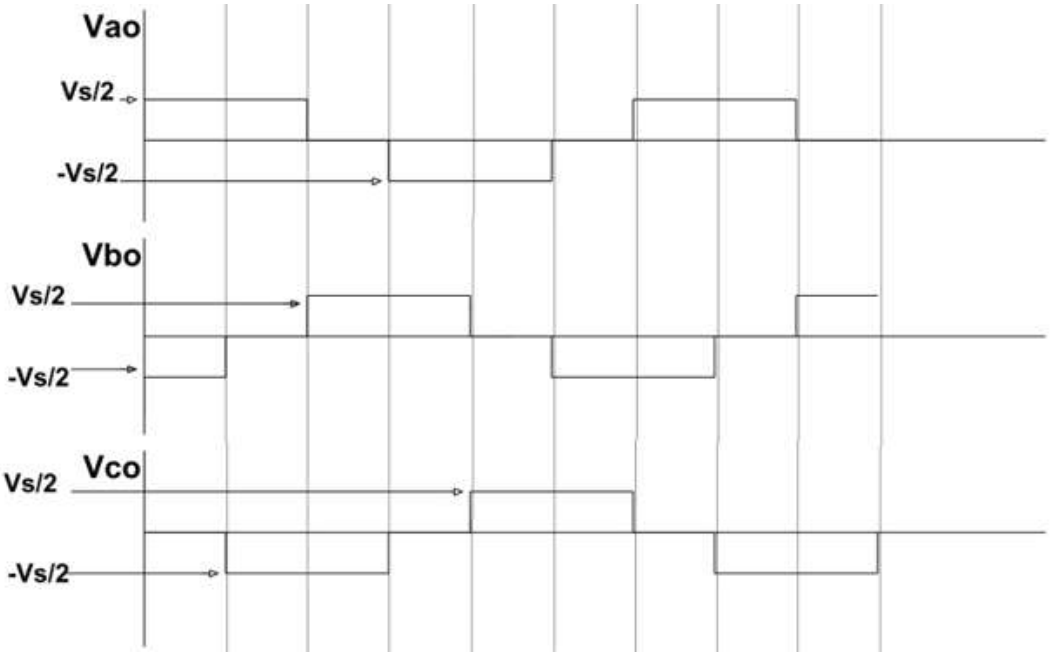

Figure 1-9: Phase to neutral voltage waveforms

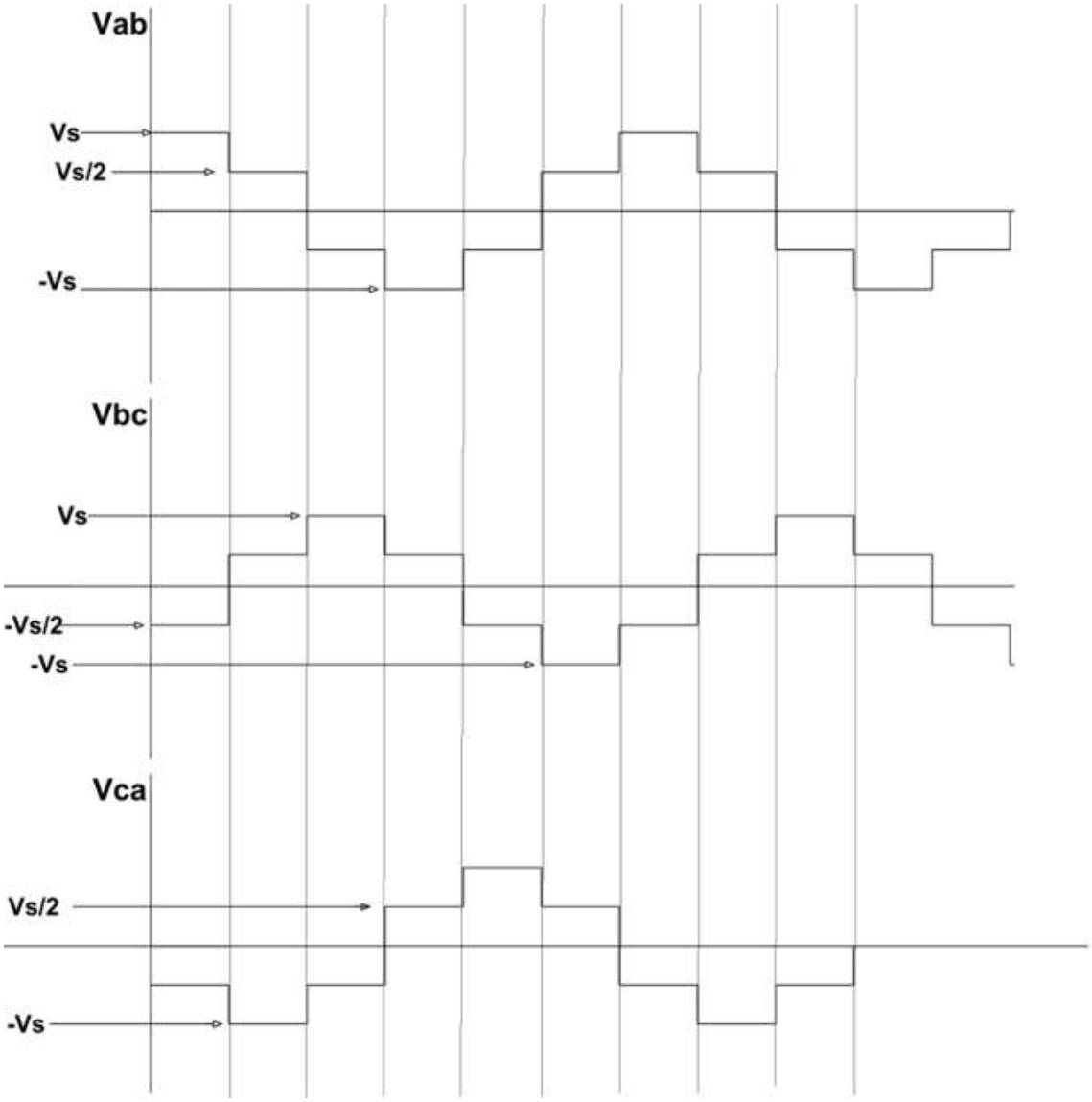

Figure 1-10: Phase to phase voltage waveforms

1.5 Switching Techniques for Control of Three Phase Inverter

For many industrial applications it is often required to control the output voltage of the 3-phase inverters mainly to adjust the operation with the variations of DC input voltage or for the output voltage regulation of the inverter, or to obtain the voltage/frequency control for speed control application of AC motors. There are various techniques to vary the output gain of the inverter and the most efficient method for controlling output is to incorporate pulse-width modulation (PWM) control within the inverters. Commonly used techniques are:

1. Pulse Width Modulation (PWM)
2. Sinusoidal Pulse Width Modulation (SPWM)
3. Space Vector Pulse Width Modulation (SVPWM)

1.5.1 Pulse Width Modulation (PWM)

PWM is the most widely used method for controlling the output voltage of three-phase inverters. In single pulse-width modulation control, there is only one pulse per half cycle and the width of the pulse is varied, while keeping the frequency constant [6]. By changing the pulse width, the effective voltage applied to the load can be controlled. The gating signal is given in figure below.

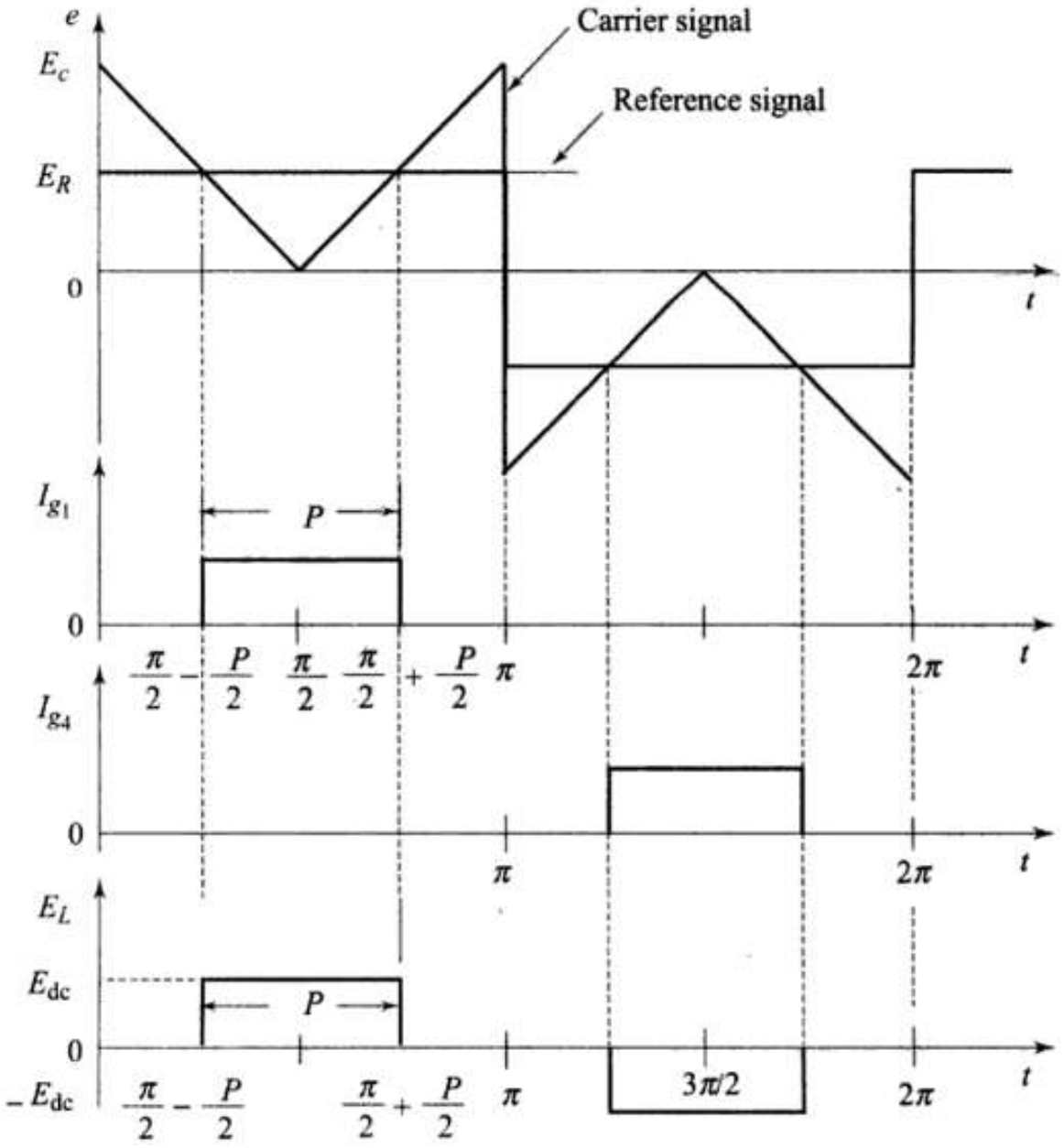

Figure 1-11: Pulse Width Modulation (PWM)

Conversely Several pulses in each half-cycle of the output voltage are generally produced to reduce the harmonic contents and to increase harmonic frequencies for reducing the size

and costs of filtering. This technique is known as multiple-pulse-width modulation. The generation of gating signals for turning on and off transistors is shown in Figure below

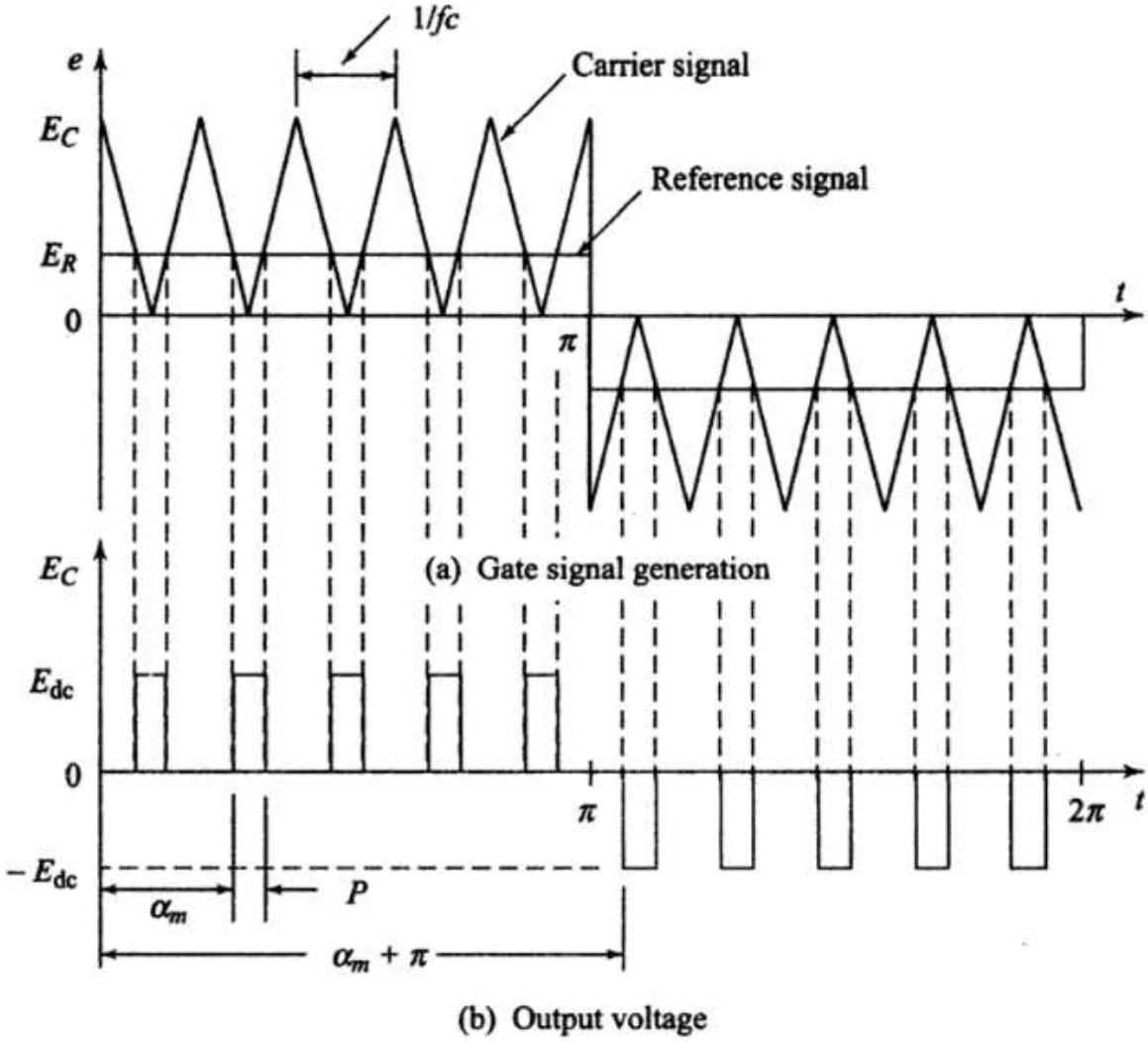

Figure 1-12: Multiple-pulse-width modulation

1.5.2 Sinusoidal Pulse Width Modulation (SPWM)

In SPWM, since the desired output voltage is a sine wave a reference sinusoidal signal is used as the reference signal. The reference sine waveform is compared with a high-frequency triangular carrier waveform. The intersection points between the two waveforms determine the switching instants of the inverter legs. This way, instead of maintaining the width of all pulses the same as in the case of multiple-pulse modulation, the width of each pulse is varied in proportion to the amplitude of a sine wave evaluated at the center of the same pulse. By adjusting the amplitude of the carrier waveform, the modulation index can be controlled, thus controlling the output voltage magnitude.

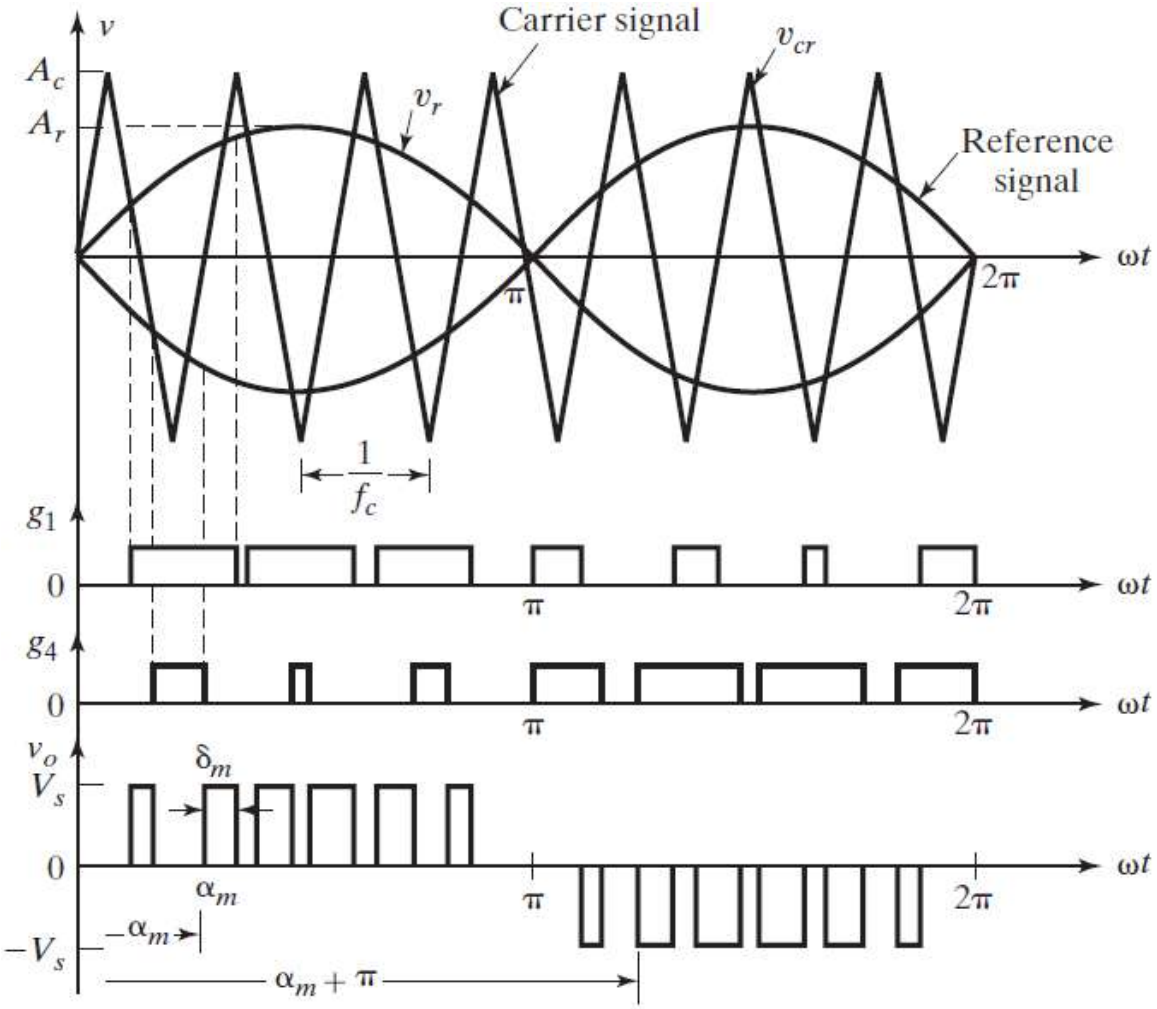

Figure 1-13: Sinusoidal Pulse Width Modulation (SPWM)

1.5.3 Space Vector Pulse Width Modulation (SVPWM)

Space Vector Pulse Width Modulation (SVPWM) is a more advanced technique that offers better utilization of the DC voltage source and improved harmonic performance. Unlike traditional Pulse Width Modulation (PWM), SVPWM optimally utilizes the available DC voltage to produce a smoother and more precise output voltage waveform. By dividing the reference voltage vector into six sectors and adjusting the duty cycles of the switching devices, SVPWM generates the optimal voltage vector, ensuring better harmonic performance and improved power conversion efficiency. This technique has gained prominence due to its ability to balance high-quality output with reduced losses, making it a preferred choice for efficiently control AC motor drives, renewable energy systems, and industrial applications.

Triangular approach can be used to implement space vector pulse width modulation. It is very easy to implement and is usually known as conventional space vector pulse width

modulation. To implement conventional SVPWM, consider the figure It shows the switching times for sector 1, here if average of the pole voltages is taken under consideration for that particular sub-cycle, then the values for all the three phases are found, and particular average values respective to all the three phases are obtained. These are denoted by $V_{AN(av)}$, $V_{BN(av)}$ and $V_{CN(av)}$. Now by comparing it with a triangular wave, results produce the same switching instances for a sub-cycle. This approach is same as that of the sine triangular PWM approach, the difference between the two lies in the application of zero vectors, for the sine triangular PWM time for application of positive (111) and negative (000) zero vectors is not the same, however, for the space vector PWM it's the same. Therefore, in-order to make this approach of conventional PWM equivalent to that of the space vector PWM (that was derived earlier) the time of application of both zero vectors (111 and 000) should be made equal. This can be done by adding some common mode to the averaged signals.

Sector	Upper Switches (S_1, S_3, S_5)	Lower Switches (S_4, S_6, S_2)
1	$S_1 = T_1 + T_2 + T_0/2$ $S_3 = T_2 + T_0/2$ $S_5 = T_0/2$	$S_4 = T_0/2$ $S_6 = T_1 + T_0/2$ $S_2 = T_1+T_2+T_0/2$
2	$S_1 = T_1 + T_0/2$ $S_3 = T_1 + T_2 + T_0/2$ $S_5 = T_0/2$	$S_4 = T_2 + T_0/2$ $S_6 = T_0/2$ $S_2 = T_1+T_2+T_0/2$
3	$S_1 = T_0/2$ $S_3 = T_1 + T_2 + T_0/2$ $S_5 = T_2 + T_0/2$	$S_4 = T_1+T_2+T_0/2$ $S_6 = T_0/2$ $S_2 = T_1 + T_0/2$
4	$S_1 = T_0/2$ $S_3 = T_1 + T_0/2$ $S_5 = T_1 + T_2 + T_0/2$	$S_4 = T_1+T_2+T_0/2$ $S_6 = T_2 + T_0/2$ $S_2 = T_0/2$
5	$S_1 = T_2 + T_0/2$ $S_3 = T_0/2$ $S_5 = T_1 + T_2 + T_0/2$	$S_4 = T_1 + T_0/2$ $S_6 = T_1+T_2+T_0/2$ $S_2 = T_0/2$
6	$S_1 = T_1 + T_2 + T_0/2$ $S_3 = T_0/2$ $S_5 = T_1 + T_0/2$	$S_4 = T_0/2$ $S_6 = T_1+T_2+T_0/2$ $S_2 = T_2 + T_0/2$

Figure 1-14: Switching sequence of Space Vector Pulse Width Modulation (SVPWM)

1.6 Description of the Components

The features of the components utilized to build the system will be explained with their figures underneath this section. The components discussed here are of several types, including electrical, electronic, active, and passive components [11].

1.6.1 Details of Components

1. MOSFET
2. Gate Driver
3. Diode
4. Three-Phase Induction Motor

1.6.2 MOSFET

MOSFET stands for Metal Oxide Semiconductor Field Effect Transistor, and it is a critical component in high-frequency, high-efficiency switching applications in the electronics industry. Surprisingly, FET technology was conceived in the 1930s, around 20 years before the bipolar transistor. The first signal-level FET transistors were produced in the late 1950s, and power MOSFETs became accessible in the mid-1970s. Millions of MOSFET transistors are now embedded in modern electronic components ranging from microprocessors to "discrete" power transistors.

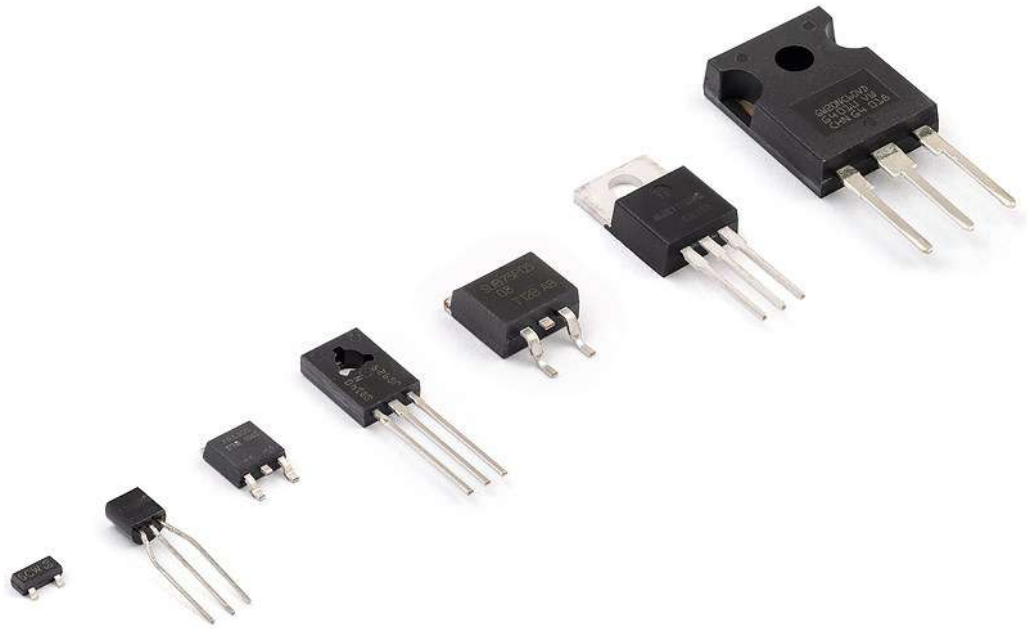

Figure 1-15: Different types of MOSFETs

BJT and MOSFET work on the same concept. They are both charge-controlled devices, which means that their output current is proportional to the charge in the semiconductor material, which is controlled by the control electrode. Both types of transistors, when used as switches, require a low-impedance source capable of delivering and draining enough current to allow for rapid charging and discharging of the control charge. This guarantees quick switching performance.

Contrary to a common misconception, MOSFETs must be driven with equal intensity during turn-on and turn-off as bipolar transistors to achieve comparable switching speeds. Theoretically, the switching speeds of both types are nearly identical, determined by the time it takes for charge carriers to move across the semiconductor region. In power devices, this time typically ranges from about 20 to 200 picoseconds, depending on the transistor's size.

MOSFETs are easier to drive because their control electrode (gate) is isolated from the current-conducting silicon. Unlike BJTs, MOSFETs do not require a continuous ON current once they are turned on. Once activated, the MOSFET's drive current becomes practically negligible.

Additionally, MOSFETs have reduced controlling charge and storage time compared to BJTs. This eliminates the design trade-off between on-state voltage drop and turn-off time. As a result, MOSFET technology enables much simpler and more efficient drive circuits, leading to significant economic benefits compared to using bipolar devices. The reduced complexity and improved efficiency make MOSFETs a preferred choice in various applications, including power electronics and switching circuits.

MOSFETs can be categorized into three basic device types. These are illustrated below:

- **Double-diffused type:** In the 1970s, double-diffused MOS transistors were introduced, primarily for power applications. Over the years, they have undergone continuous advancements and improvements. The implementation of polycrystalline silicon gate structures and self-aligning processes has played a crucial role in enabling higher-density integration and rapid reduction in capacitances within these transistors. These developments have significantly enhanced the performance and efficiency of double-diffused MOS transistors, making them more suitable for a wide range of power-related applications.

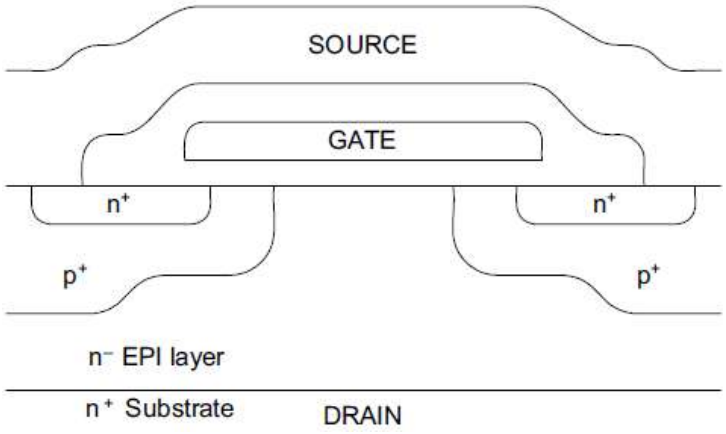

Figure 1-16: Double-diffused type MOSFET

- **Trench type:** The introduction of V-groove or trench technology marked a significant advancement in power MOSFET devices, allowing for a higher cell density and improved performance. However, these benefits do come with a trade-off, as trench MOS devices are more challenging and complex to manufacture.

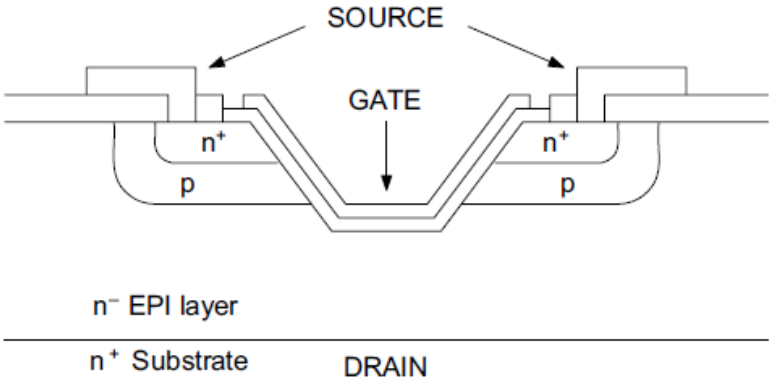

Figure 1-17: Trench type MOSFET

- **Lateral type:** Lateral power MOSFETs have noticeably reduced capacitances, resulting in faster switching speeds and a significant reduction in the required gate drive power.

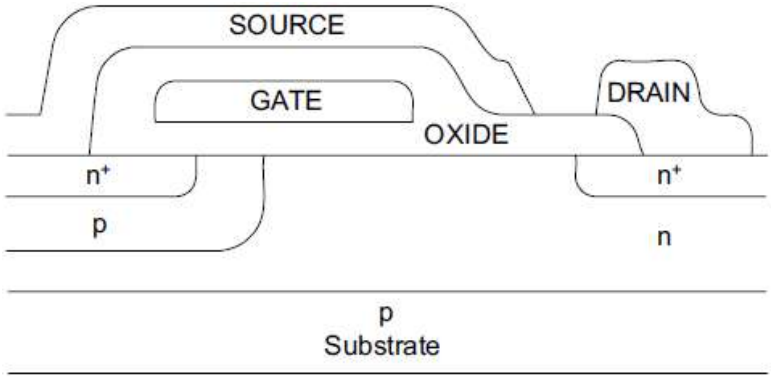

Figure 1-18: Lateral type MOSFET

1.6.3 Gate Driver

A gate driver serves as a power amplifier, responsible for transforming a low-power input received from a controller IC into a high-current output, which is utilized to drive the gate of a high-power transistor, like an IGBT or power MOSFET. Gate drivers can come in two forms: integrated on-chip or as standalone modules. An integrated gate driver IC is responsible for linking control signals to power switches like IGBTs and MOSFETs. Utilizing an integrated gate-driver solution offers numerous advantages over discretely implemented gate-drive solutions. It simplifies the design process, reduces development time, minimizes the bill of materials (BOM), and saves board space, all while enhancing overall reliability.

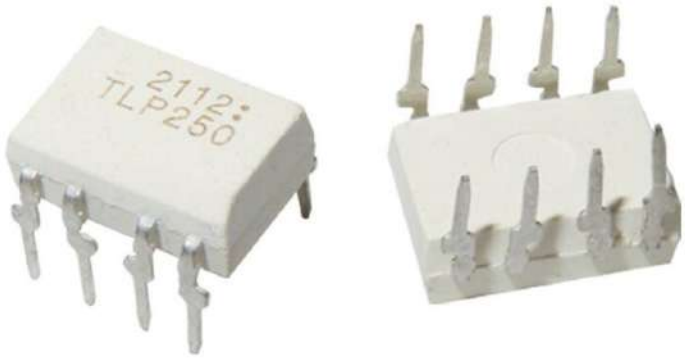

Figure 1-19: Opto-coupler gate driving IC

Unlike BJTs, MOSFETs don't necessitate a continuous power supply when they remain in an unswitched state. The MOSFET's gate terminal is isolated and acts as a capacitor (gate capacitor), which needs to be charged or discharged each time the MOSFET is switched on or off. For the transistor to turn on, the gate capacitor must be charged to reach the required specific gate voltage with reference to its source voltage. Similarly, when turning off the transistor, the charge must be dissipated, leading to the draining of the gate capacitor.

For both functional and safety reasons, gate drive circuits are frequently required to provide electrical isolation between the control circuit and the switching circuit. It also safeguards low-voltage electronics from damage caused by failures in the high-power side circuit and human mistakes on the control side. The electrical isolation of separate functional circuits in a system avoids a direct conduction path between them and permits individual circuits to have different ground potentials. Signal and power can still be transmitted between separate circuits using inductive, capacitive, or optical means.

To create isolated gate drivers, there are two prominent methods: magnetic (using gate drive transformers) and optical (using an optocoupler).

1.6.4 Diode

A diode is a two-terminal device or electronic component that conducts only in one direction. It primarily provides zero resistance to current flow in the forward direction and infinite resistance in the reverse direction. The anode and cathode are the two terminals. Anode terminals should have a higher potential than cathode terminals. A crystalline piece of semiconductor material with a p-n junction attached to two terminals is the most common type of semiconductor diode. The majority of diodes are composed of silicon; however, selenium and germanium are also used on occasion.

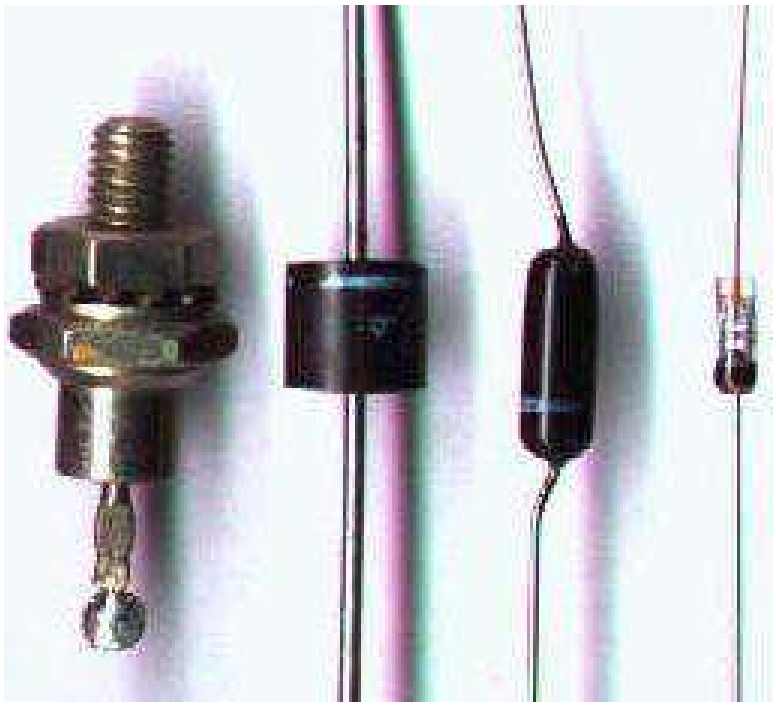

Figure 1-20: Different types of diodes

1.6.5 Capacitor

Capacitors are basic electronic components that are utilized in a vast variety of electrical and electronic systems. They use an electric field to store electrical energy. A battery, on the other hand, stores and releases electrical energy through chemical processes. It may be quickly discharged but slow to charge. A capacitor stores electrical energy temporarily by distributing charged particles on (usually two) plates to generate a potential difference. A capacitor can charge faster than a battery and discharge all of its energy much more quickly.

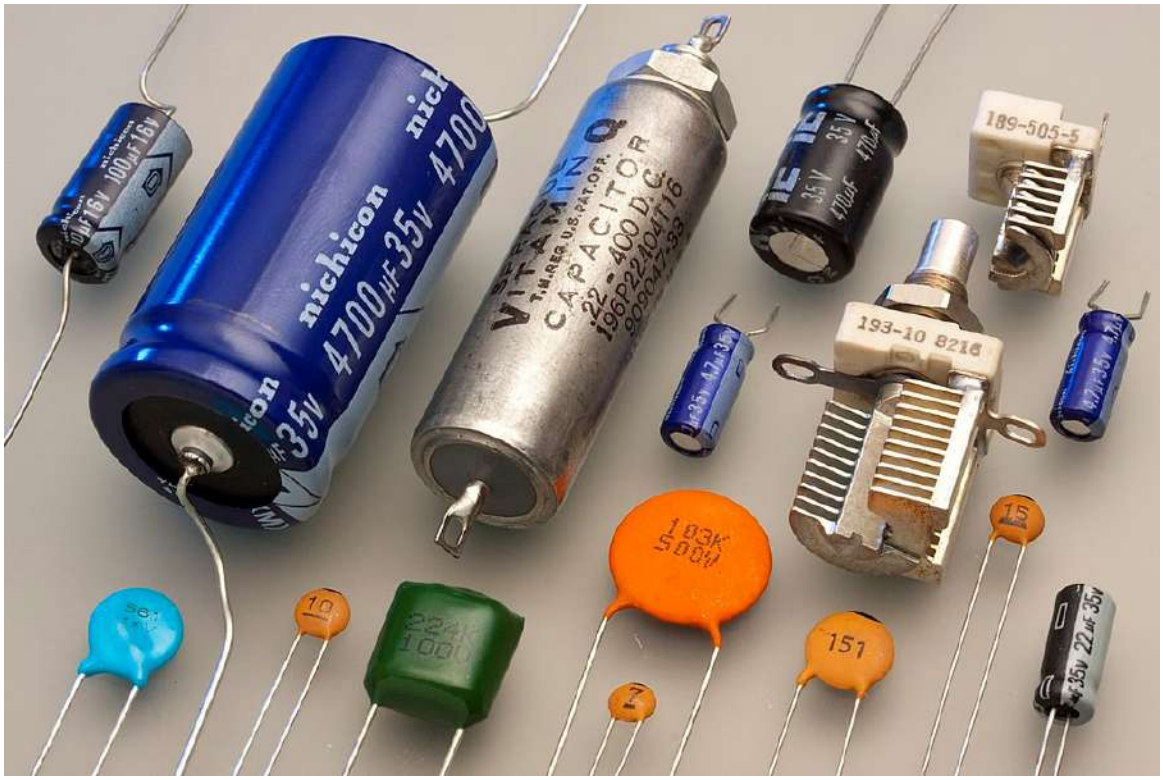

Figure 1-21: Some commonly used capacitor

1.6.6 Three-Phase Induction Motor

The induction motor is one of the most widely used electrical motors in various industrial, commercial, and residential applications. It is a type of AC (alternating current) motor that operates based on the principle of electromagnetic induction.

An induction motor consists of two main parts - the stator and the rotor. The stator is the stationary part of the motor and contains the stator winding, which is supplied with AC voltage. The rotor is the rotating part and can be either wound with rotor windings (slip-ring) or cage rotor (squirrel cage). Most induction motors use squirrel-cage rotors due to their simplicity and robustness. When AC voltage is applied to the stator winding, it creates a rotating magnetic field. This rotating magnetic field induces a current in the rotor, which in turn creates a magnetic field in the rotor. The interaction between the rotating magnetic field in the stator and the induced magnetic field in the rotor generates torque, causing the rotor to rotate.

The speed of an induction motor is determined by the frequency of the AC voltage and the number of poles in the motor. The speed is relatively fixed and depends on the synchronous speed, which can be calculated using the formula:

$$Synchronous\ Speed\ (RPM)\ = \frac{120 \times Frequency}{Number\ of\ Poles}$$

Speed can be controlled by varying the voltage supplied to the stator winding. However, this method is less efficient since it can lead to reduced torque output and increased heat losses in the motor. Another method to control the motor's speed is by adjusting the frequency and voltage of the power supplied to the motor. By changing the frequency of the AC voltage, the synchronous speed of the motor can be varied, which, in turn, alters the motor's actual speed. For this purpose, variable frequency drives (VFDs) are widely used in industrial applications for precise speed control, energy savings, and smooth starting and stopping.

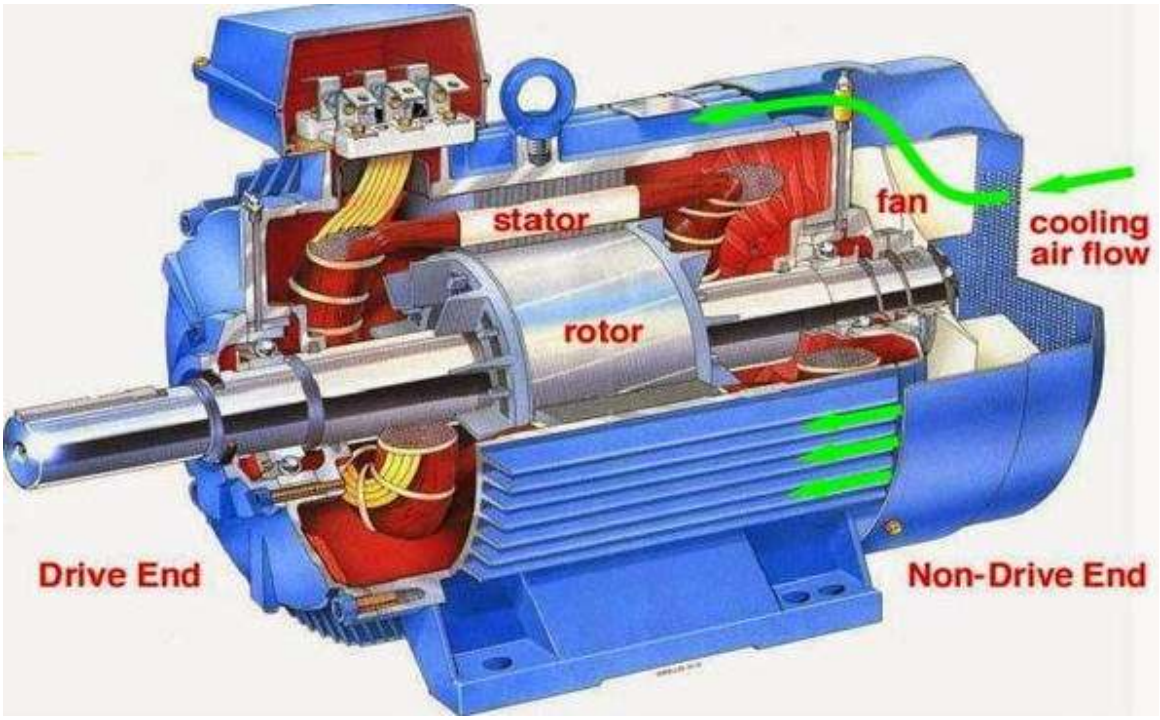

Figure 1-22: Cutout view of induction motor

Induction motors are known for their high efficiency and reliability. They have a simple and rugged design, which makes them easy to manufacture and maintain. Additionally, they do not require brushes or slip rings, reducing wear and maintenance needs.

1.7 Introduction to Controller

1.7.1 Arduino Uno

The Arduino Uno is an open-source microcontroller board based on the ATmega328P. One of the most well-known and frequently used boards created by Arduino.cc, it is ideal for hobbyists and beginners who want to explore electronics and programming. The Arduino

Uno is like a tiny computer with special powers. It can sense the world around it using various sensors, such as temperature, light, or motion sensors. It can also control other devices, like turning on lights, moving motors, or making sounds. It has digital pins that can be used to read or write digital signals (like on/off) and analog pins that can read continuous signals (like varying voltage levels) [7].

The board can be powered either through a USB connection or an external power supply. It features a USB interface, enabling users to easily upload their programs (known as sketches) from their computers to the board. The Arduino Uno is compatible with the Arduino Integrated Development Environment (IDE), which is a user-friendly software that allows users to write, compile, and upload code to the board.

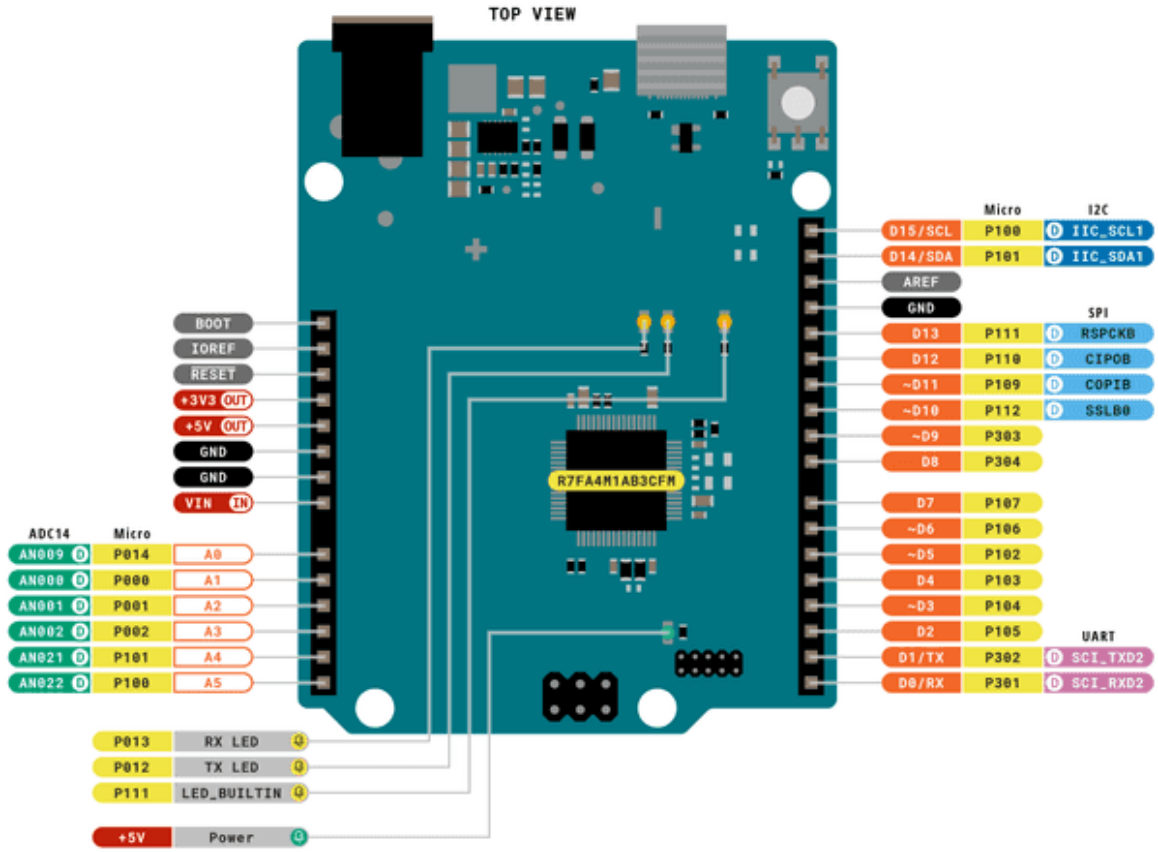

Figure 1-23: Pinout configuration of Arduino Uno

The Arduino Uno is incredibly versatile and has found applications in a wide range of projects, including home automation, robotics, IoT (Internet of Things) devices, environmental monitoring, interactive art installations, and more. Its simplicity, extensive community support, and a vast collection of libraries and examples make it an excellent platform for learning and exploring electronics and programming.

Key features of the Arduino Uno include:

- **Microcontroller:** The Arduino Uno is powered by the ATmega328P microcontroller, operating at 16MHz. It has 32KB of flash memory, 2KB of SRAM, and 1KB of EEPROM, providing sufficient resources for running various projects.
- **Digital and Analog I/O:** The board offers 14 digital input/output pins, with 6 of them capable of providing pulse-width modulation (PWM) output. Additionally, there are 6 analog input pins, enabling connections with a variety of sensors and devices.
- **Communication Interfaces:** The Arduino Uno supports several communication interfaces, including one hardware UART (Serial), one hardware I2C/TWI interface, and one hardware SPI interface. These interfaces facilitate seamless communication with other devices, such as computers, sensors, and displays.
- **Power Supply:** The board can be powered via a USB connection or an external power supply (7-12V DC). It features a built-in voltage regulator, ensuring a stable 5V supply for the board and connected components.
- **Compatibility:** The Arduino Uno is fully compatible with the Arduino IDE (Integrated Development Environment), allowing users to write, compile, and upload code easily. The vast library of community-contributed code and projects is readily accessible to users.
- **Shields:** Arduino Uno boards have a standardized form factor, making them compatible with various expansion boards called "shields." These shields provide pre-built modules for specific functionalities, enabling quick and easy prototyping and project development.

1.7.2 Arduino Mega

Arduino Mega is another popular microcontroller board developed by Arduino.cc. It is an enhanced version of the standard Arduino boards, offering a more extensive range of input/output pins and increased memory capacity, making it suitable for more complex and demanding projects compared to the Arduino Uno.

The Arduino Mega is based on the ATmega2560 microcontroller, operating at 16MHz. It features 256KB of flash memory, 8KB of SRAM, and 4KB of EEPROM, providing ample resources for running more extensive and sophisticated programs.

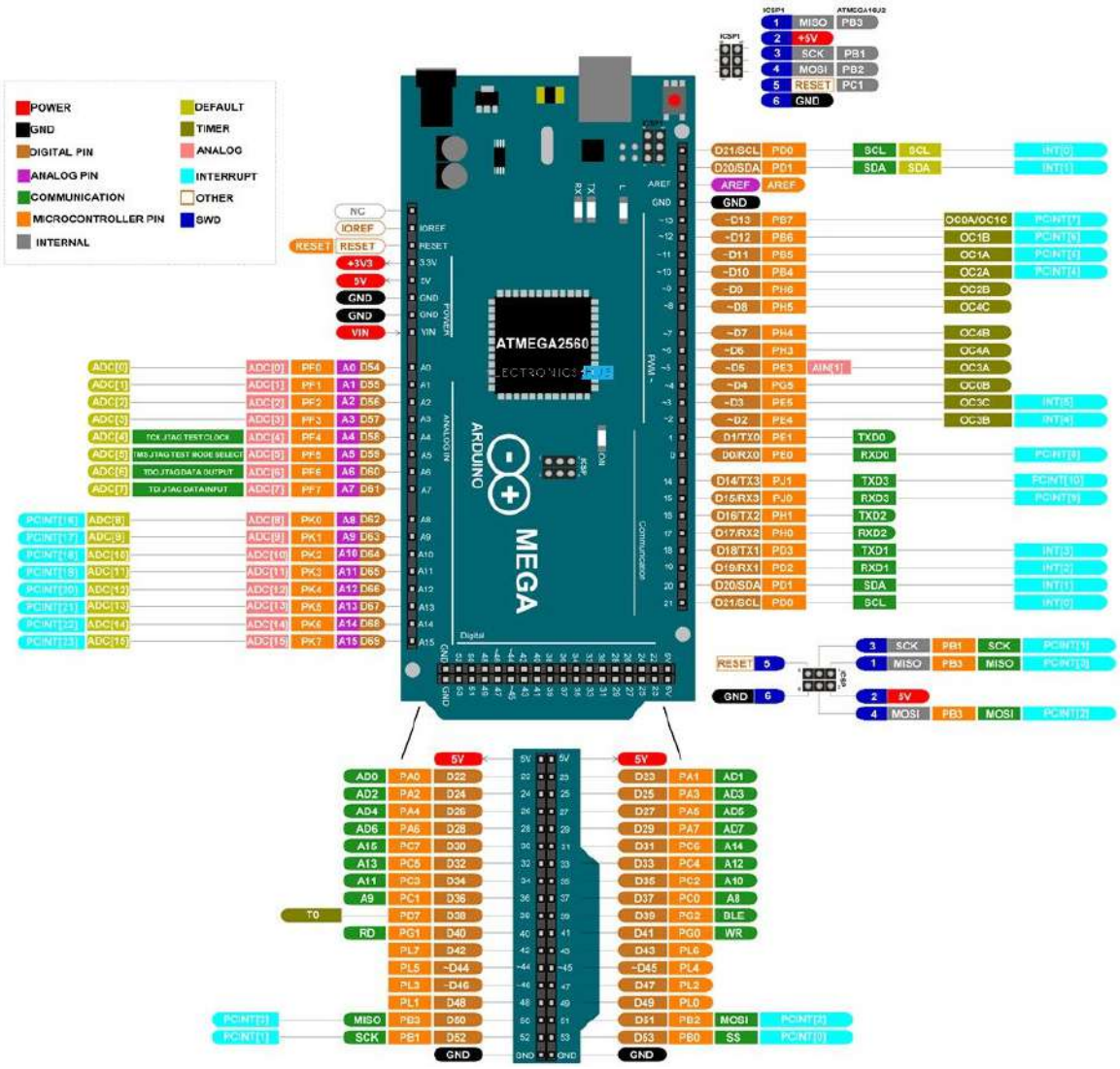

Figure 1-24: Pinout configuration of Arduino MEGA

Key features of the Arduino Mega include:

- **Microcontroller:** The Arduino Mega is powered by the ATmega2560 microcontroller, which operates at 16MHz and has 256KB of flash memory, 8KB of SRAM, and 4KB of EEPROM. This provides ample resources for running more extensive and sophisticated programs.
- **Digital and Analog I/O:** The board boasts 54 digital input/output pins, of which 15 can be used for pulse-width modulation (PWM) output. Additionally, there are 16 analog input pins, allowing for a wide range of sensor connections and data acquisition.
- **Communication Interfaces:** The Arduino Mega supports multiple communication interfaces, including four hardware UARTs (Serial ports), one hardware USART

(Serial1), and two hardware I2C/TWI interfaces. It also features one hardware SPI port, which facilitates communication with other devices like sensors and displays.

- **Power Supply:** The board can be powered through the USB connection or an external power supply (7-12V DC). It also has a built-in voltage regulator, which ensures a stable 5V supply for the board and connected components.
- **Compatibility:** The Arduino Mega is fully compatible with the Arduino IDE (Integrated Development Environment), which simplifies programming and enables users to access a vast library of community-contributed code and projects.
- **Shield Compatibility:** The Arduino Mega has the same form factor as standard Arduino boards, making it compatible with most Arduino shields. This expandability allows users to augment the capabilities of the board by adding pre-built modules for various functionalities.

Due to its rich features and versatility, the Arduino Mega is a favored choice among hobbyists, educators, and professionals for projects requiring a higher number of I/O pins, increased memory, and more computational power. Its ability to handle complex tasks and interface with various devices makes it an ideal platform for robotics, automation, home automation, data logging, and many other applications in the realm of electronics and programming.

1.7.3 HMI Display

The Nextion HMI (Human-Machine Interface) display is a series of touchscreens developed by ITEAD Studio. HMI displays are user-friendly graphical interfaces that allow users to interact with electronic devices easily. The Nextion displays are designed to be versatile and user-friendly, making them popular choices in various projects and applications.

Nextion displays utilize high-quality TFT (Thin-Film Transistor) LCD screens that offer clear and vibrant colors. They are available in different sizes, ranging from small screens for portable projects to larger displays for more extensive applications. The primary method of interaction with Nextion displays is through touch. The displays are equipped with a capacitive or resistive touch panel, depending on the model, that enables users to input commands and interact with the displayed content effortlessly.

Figure 1-25: Nextion HMI LCD display

Nextion displays support various communication protocols, including UART (Serial), I2C, and RS232, to facilitate seamless integration with a wide range of microcontrollers, single-board computers, and other embedded systems. These displays come with an integrated microcontroller unit, which offloads some of the processing tasks from the main controller or microcontroller in the system. They also have a built-in EEPROM (Electrically Erasable Programmable Read-Only Memory), allowing users to store data and settings even when the power is disconnected.

Nextion also provides a user-friendly GUI (Graphical User Interface) editor software that allows users to design custom graphical interfaces without the need for complex coding. The GUI editor includes drag-and-drop components, making it accessible to both beginners and experienced developers.

1.7.4 IoT Module

The ESP32 is a popular choice for IoT (Internet of Things) and cloud applications due to its powerful features, low power consumption, and built-in Wi-Fi and Bluetooth connectivity. It enables developers to create smart and connected devices that can communicate with cloud platforms and seamlessly integrate into IoT ecosystems.

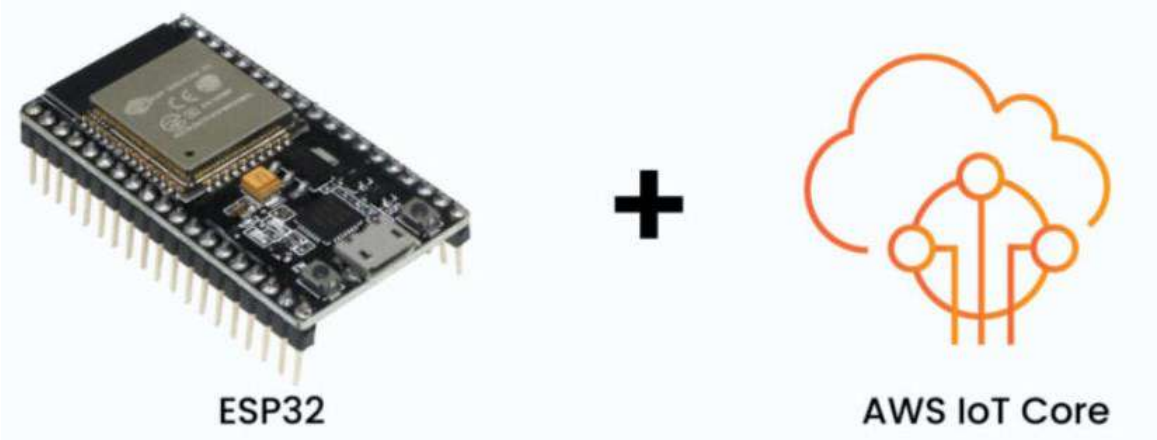

Figure 1-26: ESP32 and AWS cloud

The ESP32 can easily integrate with popular cloud platforms and IoT services, such as Amazon Web Services (AWS), Google Cloud IoT Core, Microsoft Azure IoT Hub, and many others. This enables seamless data exchange, remote monitoring, and control of IoT devices from anywhere in the world. Security is critical in IoT and cloud applications. The ESP32 supports various encryption and authentication protocols, ensuring secure communication between the device and cloud servers.

The ESP32 is designed to be power-efficient, making it suitable for battery-powered IoT devices. Its low power modes enable devices to enter sleep or deep sleep states when idle, conserving energy and extending battery life.

Chapter 2

2 LITERATURE SURVEY

The application of induction motors and Variable Frequency Drives (VFDs) in electric vehicles (EVs) equipped with smart features has garnered significant attention in recent research. This literature review aims to explore the multifaceted benefits and advancements stemming from this integration [8].

Induction motors, renowned for their reliability and robustness, have found a niche in the EV industry. Various studies highlight their suitability for EV propulsion due to high efficiency and simplified construction. Additionally, research by Akhtar et al. (2019) emphasizes the importance of induction motors' inherent regenerative braking capabilities, contributing to energy recuperation and extended range. The work of Han et al. (2020) further underscores the advantages of induction motors in improving vehicle stability and torque distribution in four-wheel-drive setups .

However, the true potential of induction motors in EVs is realized when coupled with Variable Frequency Drives (VFDs), enabling precise speed and torque control. Numerous studies underscore the significance of VFDs in enhancing energy efficiency through optimal power distribution. Moreover, the flexibility of VFDs in adjusting motor performance according to driving conditions is emphasized by research from Chen et al. (2021), contributing to smoother acceleration and improved driving experiences .

The integration of smart features in EVs has added a new dimension to this synergy. Research by Li et al. (2019) delves into the incorporation of VFDs in EVs with autonomous capabilities, where VFD-driven induction motors enable enhanced vehicle control [9]. The connectivity aspect is explored by Wang et al. (2020), showcasing how VFDs, in conjunction with smart sensors, facilitate real-time data transmission for remote diagnostics and performance monitoring .

The collective advancements in EV technology, induction motors, VFDs, and smart features are showcased in the work of Zhang et al. (2022). Their comprehensive study

demonstrates how this integration results in extended driving range, improved energy management, and seamless connectivity [10].

In conclusion, the literature supports the application of induction motors and VFDs in EVs enriched with smart features. This integration not only enhances propulsion efficiency and driving performance but also ushers in a new era of connectivity, data analysis, and autonomous capabilities, paving the way for sustainable and intelligent electric transportation.

Chapter 3

3 DESIGN, SIMULATION & HARDWARE IMPLEMENTATION

3.1 Introduction

In this chapter, the designing of proposed system will be discussed. Simulation section consists of computer simulation of variable frequency inverter in Proteus design suit simulation software. The inverter topology is simulated with optimal and easily available in market electronic components.

After simulation the initial hardware circuit is implemented. The implemented hardware circuit is tested and results are compared with simulation results. Any deviations from simulation results are rectified and final hardware circuit is implemented.

The designing of low voltage, low power three phase induction motor is also discussed in this section. The complete process, stages and parameters are examined. The newly designed motor is attached to inverter circuit.

3.2 Schematic Diagram

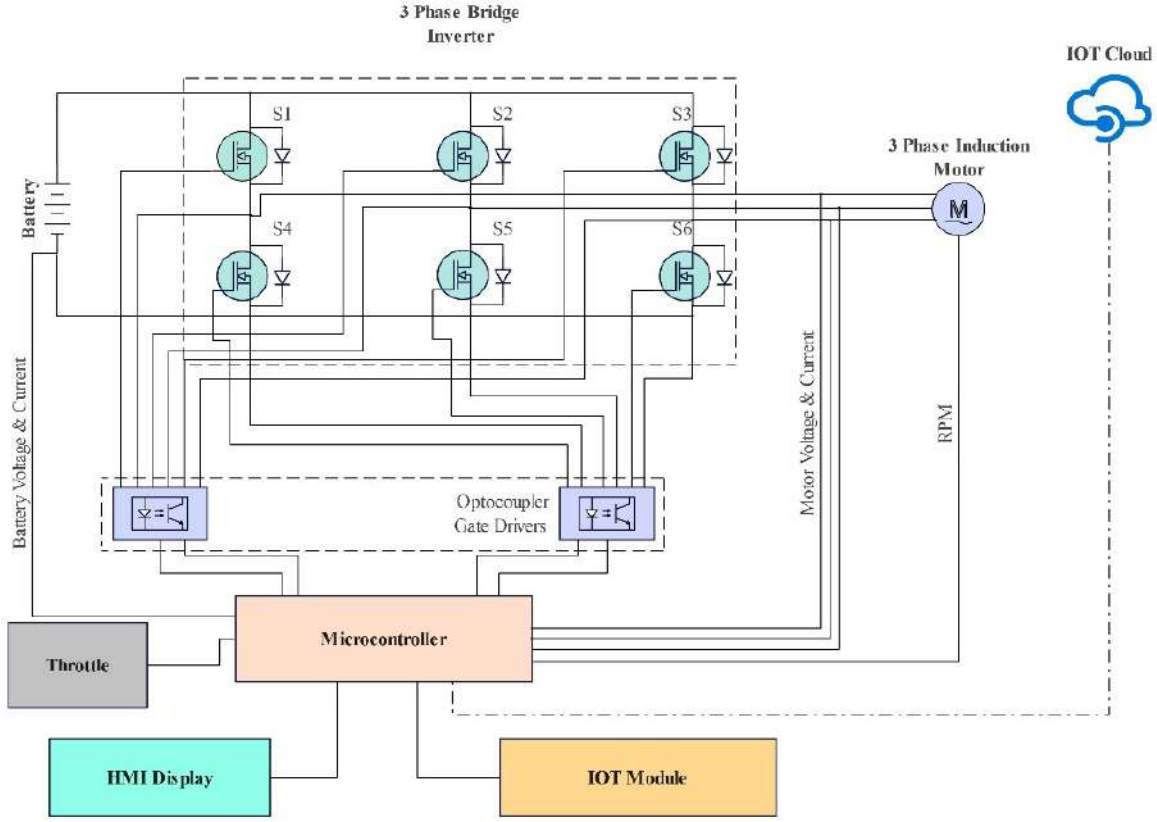

Figure 3-1: Schematic Diagram

3.3 Simulation

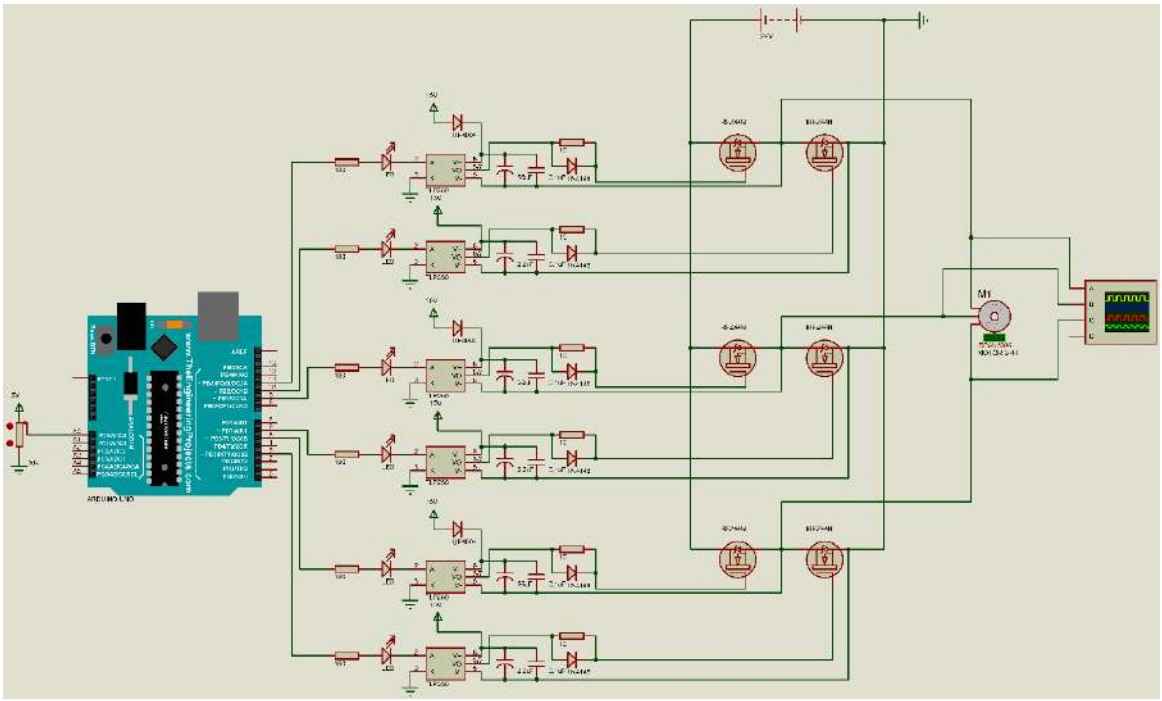

Figure 3-2: Simulation Circuit

3.4 Simulation Results

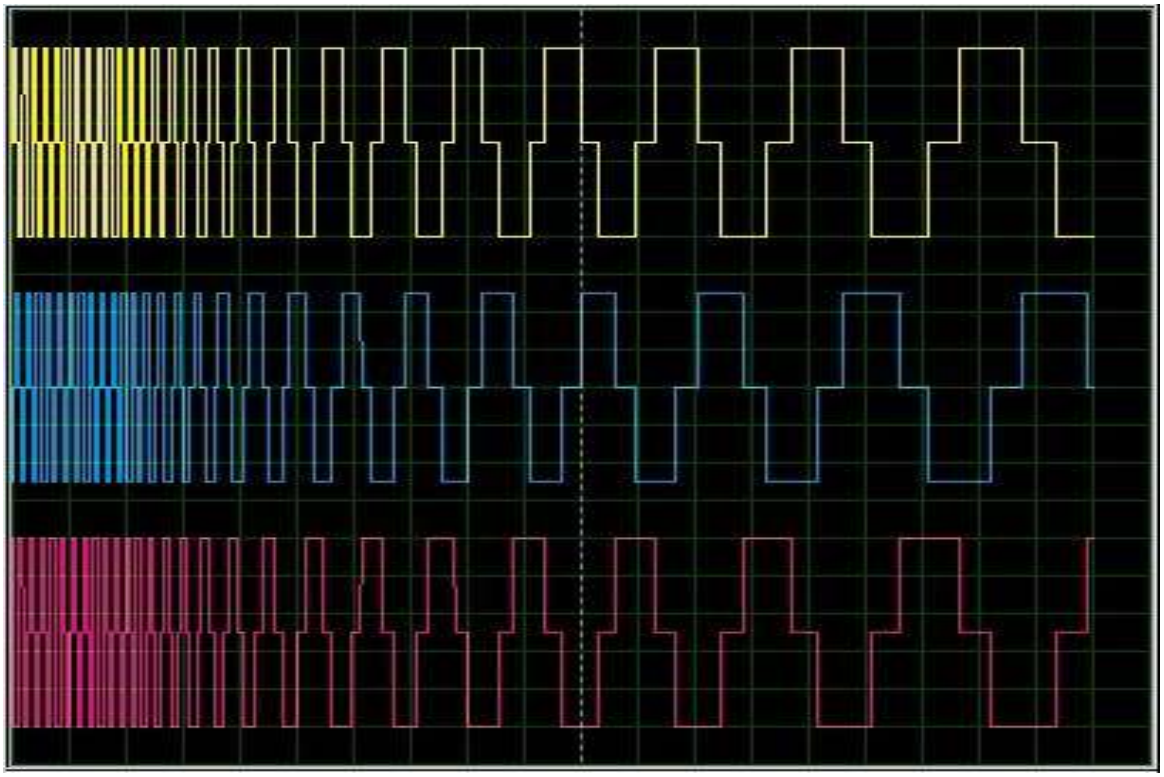

Figure 3-3: 120˚ Conduction mode, Phase to Neutral voltage

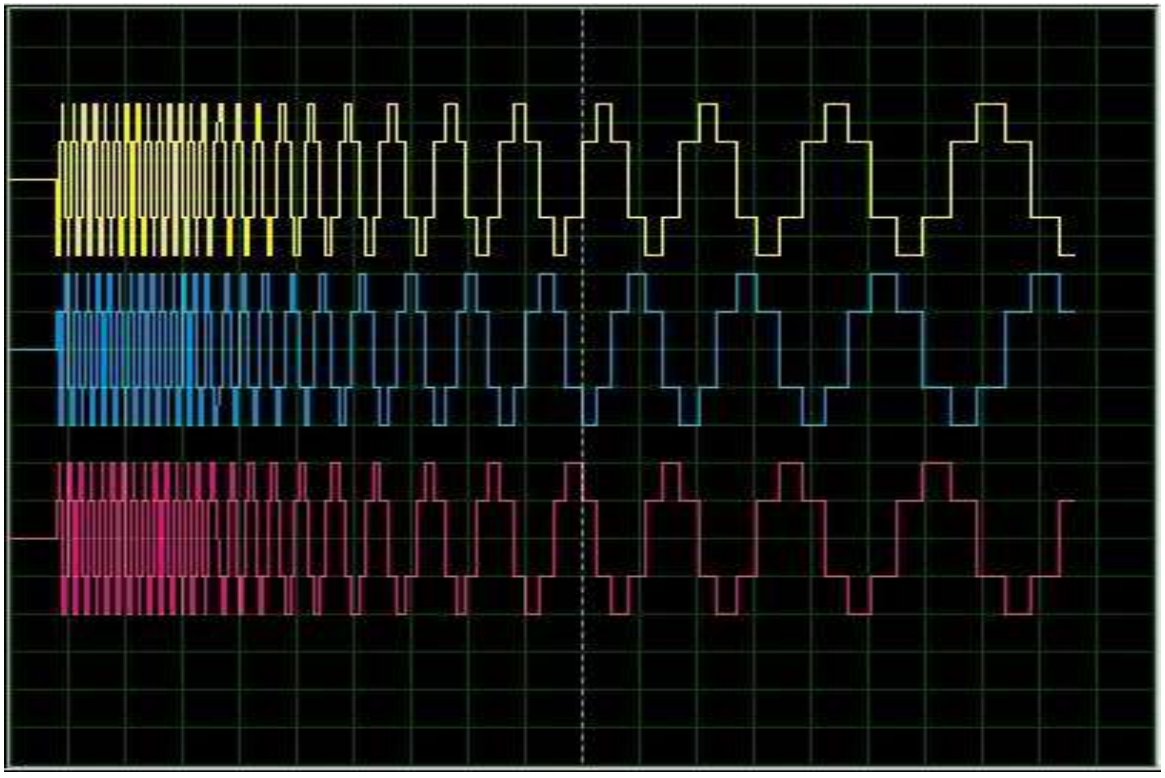

Figure 3-4: 120˚ Conduction mode, Phase to Phase voltage

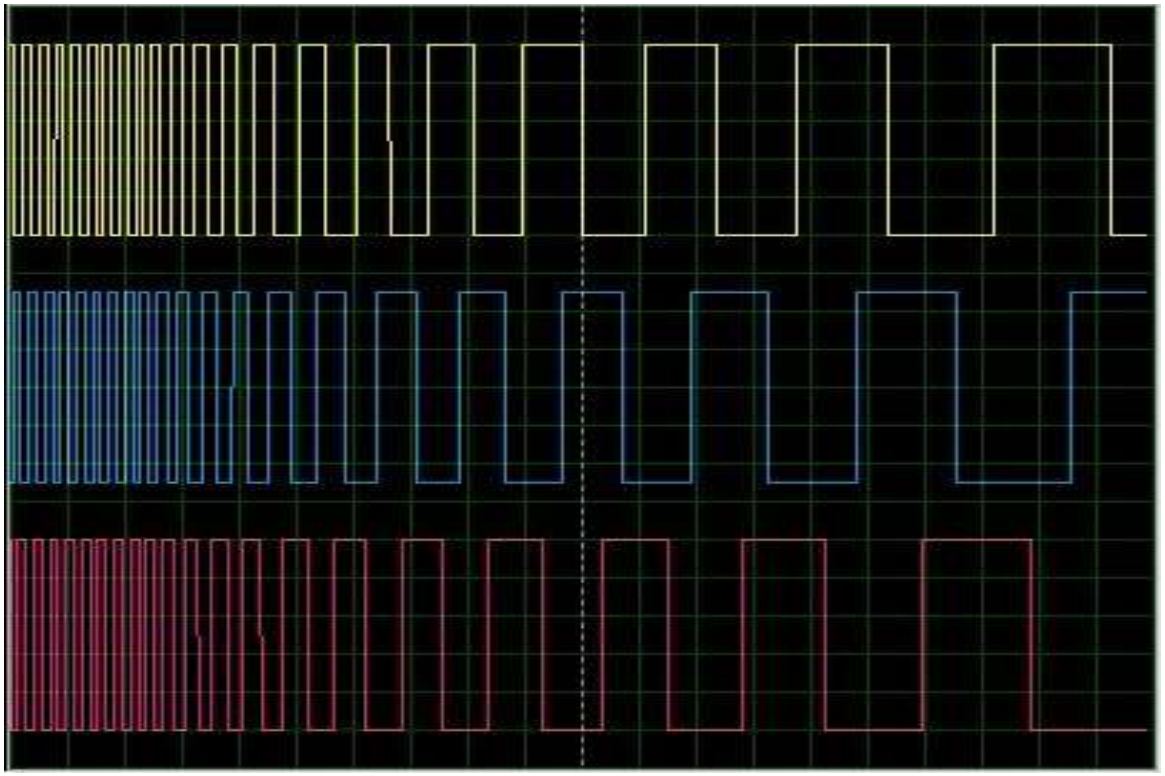

Figure 3-5: 180˚ Conduction mode, Phase to Neutral voltage

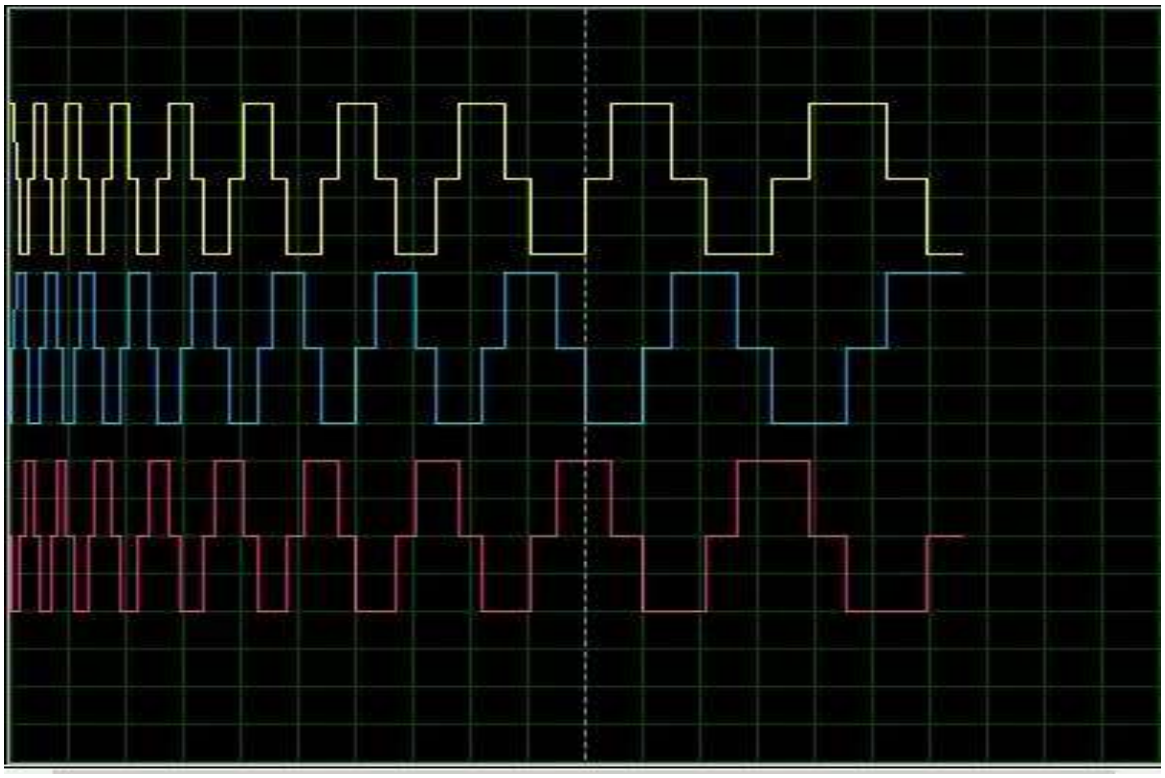

Figure 3-6: 180˚ Conduction mode, Phase to Phase voltage

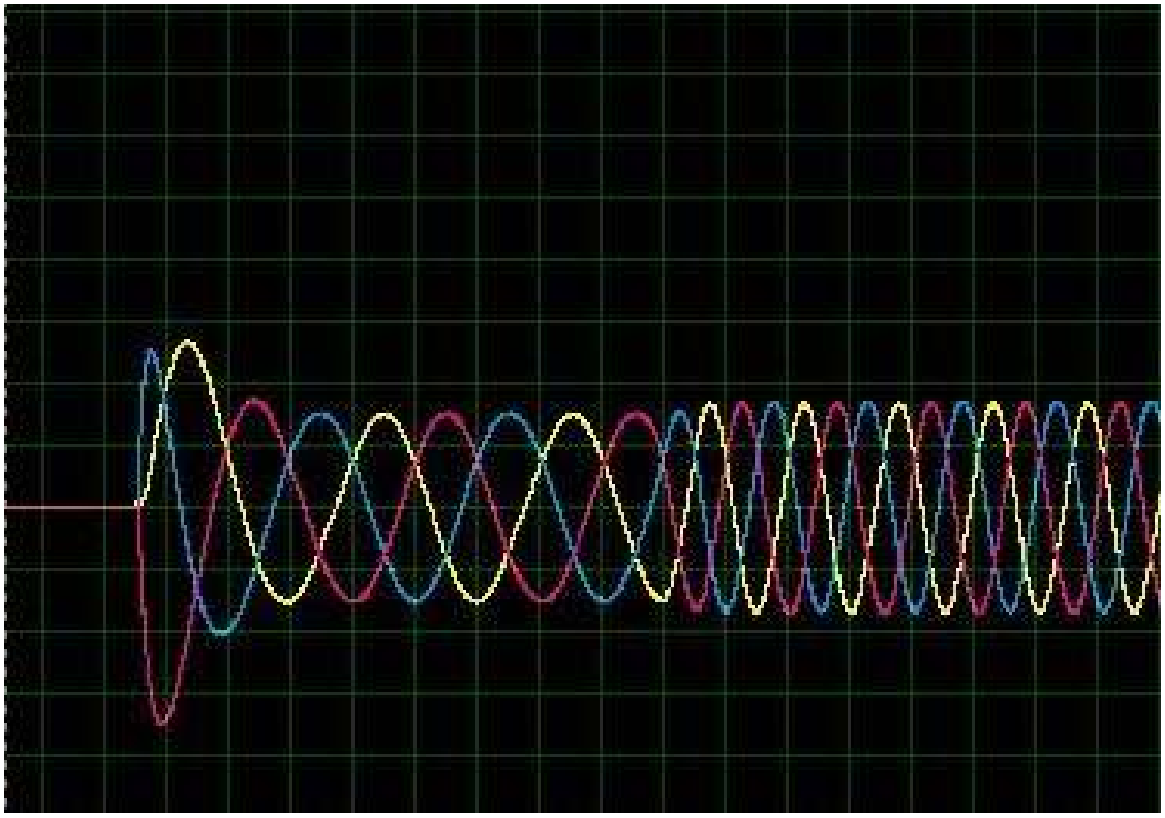

Figure 3-7: Three phase Sinusoidal waves with variable frequency

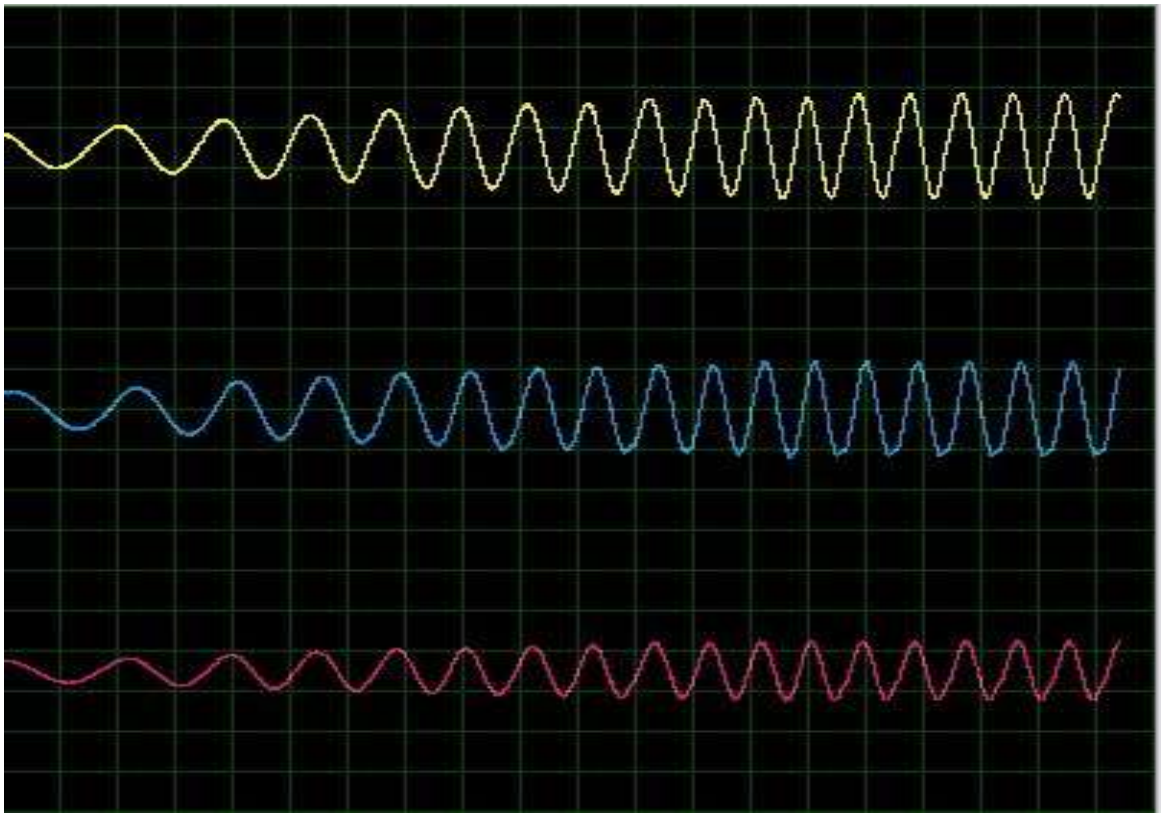

Figure 3-8: Three phase sine wave with variable frequency and amplitude

3.5 Selection of Hardware Components

Following components are used for implementation of final hardware.

- IRFZ44N MOSFETs for Three-phase bridge circuit
- TLP250 Optocoupler gate driver IC
- Bootstrap Capacitors
- Bootstrap Diode
- Filter Capacitors
- Arduino Mega 2560
- Nextion HMI display
- 24V Three-phase induction motor

3.5.1 IRFZ44N MOSFETs

The IRFZ44N is a popular N-channel power MOSFET used in various electronic applications. It is designed to handle high current and voltage, making it suitable for power switching and amplification tasks. The IRFZ44N is widely used in various applications such as motor control, LED lighting, power supplies, and automotive circuits, among others. Its ability to handle high current and voltage, combined with its relatively low on-resistance, makes it an excellent choice for switching high-power loads efficiently. However, it is important to consider appropriate heat dissipation measures when using the IRFZ44N in high-power applications to prevent overheating and ensure reliable operation.

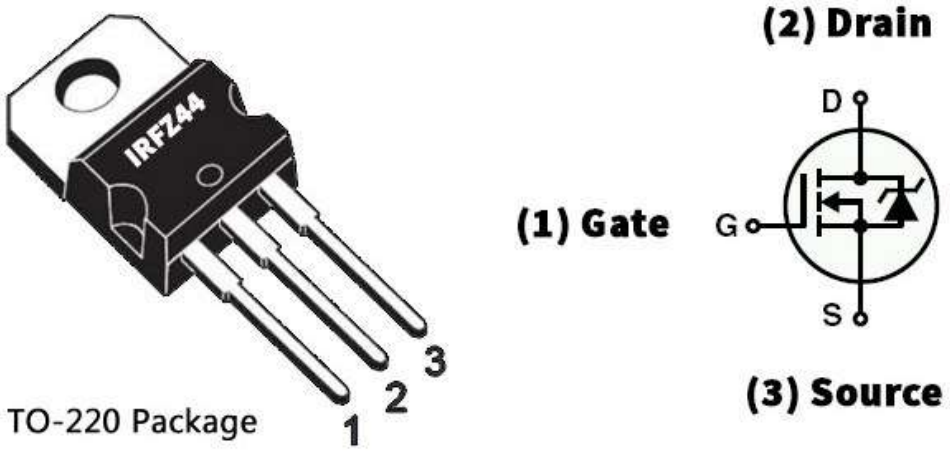

Figure 3-9: IRFZ44N MOSFET Pinout configuration

Key specifications of the IRFZ44N include:

- Type: N-Channel MOSFET
- Drain-Source Voltage (V_{DS}): Typically rated for around 55V
- Continuous Drain Current (I_D): Typically rated for several tens of amperes with continuous drain current is 49A at 25°C, while peak or pulsed drain current is 160A.

- On-Resistance ($R_{DS(ON)}$): Ultra Low On-Resistance, when fully turned on its only 17.5mΩ, which minimizes power dissipation and the voltage drop across the MOSFET during operation.
- Gate Threshold Voltage ($V_{GS(th)}$): The voltage at which the MOSFET starts to conduct when the gate voltage is applied. $V_{GS(th)}$ at minimum is 2V while the maximum is 4.5V. Because of the low threshold voltage, the IRFZ44N N-channel MOSFET transistor works with Arduino in most cases.
- Power Dissipation: The power dissipation is at 94W Max.
- Switching time: The rise time is around 60ns, while the fall time is approximately 45ns.
- Package: The IRFZ44N is commonly available in a TO-220 package, which is easy to mount on a heat sink for better thermal performance.

3.5.2 TLP250 Optocoupler gate driver IC

The TOSHIBA TLP250 is a widely used gate driver IC that belongs to the optocoupler family which consists of an infrared emitting diode and an integrated photodetector. It serves as an isolated interface between low-power control circuits and high-power devices, such as IGBTs and power MOSFETs. The TLP250 employs an optically coupled configuration, ensuring electrical isolation between its input and output. This gate driver offers several advantages, including high-speed operation, excellent noise immunity, and a wide operating voltage range. The TLP250 is designed to provide reliable and efficient switching performance, making it suitable for various applications, such as motor drives, power inverters, industrial automation, and power supply systems.

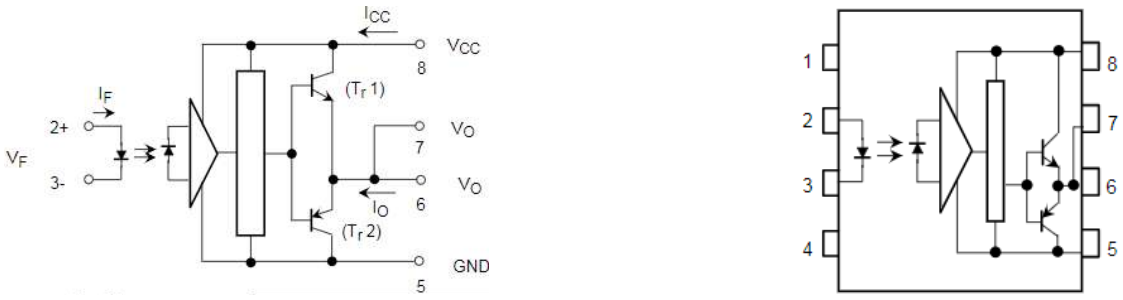

Figure 3-10: TPL 250 Pinout configuration

One of the key features of the TLP250 is its ability to protect sensitive control circuits from voltage spikes and transients that may occur in high-power switching applications. The optocoupler inside the TLP250 ensures that the control circuit remains isolated from

potential disturbances and voltage surges present on the high-power side. With its compact and easy-to-implement design, the TLP250 simplifies gate driving requirements, reducing design complexity and overall development time. Engineers often choose the TLP250 gate driver for its reliability, performance, and enhanced safety features, making it a popular choice in numerous power electronics applications across various industries.

The following are the notable characteristics and schematic with pin configuration:

- Input threshold current: 5mA(max)
- Supply current: 11mA(max)
- Supply voltage: 10-35V
- Output current: ±1.5A (max)
- Switching time: 0.5μs(max)
- Isolation voltage: 2500Vrms(min)

3.5.3 Bootstrap Capacitor, Bootstrap Diode & Filter Capacitor

The ultra-fast diodes are used in this circuit as free-wheeling in an anti-parallel arrangement with switching transistors. They are employed to safeguard the circuit from irreversible damage produced due to sudden drops in the current flowing through the circuit. It is also known as a flyback diode since it connects across the inductor to remove the flyback voltage created across it. They are also used in the bootstrap circuit with a capacitor as a bootstrap diode-capacitor set with a MOSFET gate driver circuit.

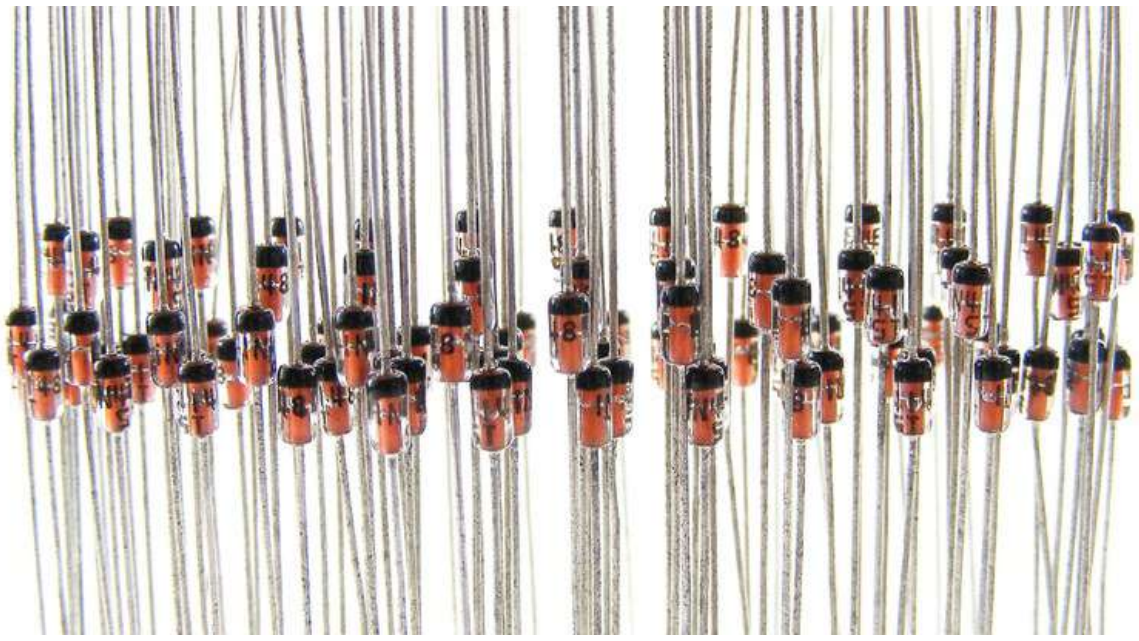

Figure 3-11: Ultra-fast Diodes 1N4148

In a bootstrap gate driver circuit, capacitors are used to generate a voltage higher than the input voltage to drive the high-side MOSFET or IGBT's gate efficiently. This technique is

commonly employed in high-side gate driver circuits for half-bridge and full-bridge configurations, where the high-side switch is not directly connected to the ground reference.

Figure 3-12: Tantalum capacitors as bootstrap capacitor

3.5.4 Designing of three phase motor

Before designing of three phase motor information about its electrical and physical parameters are noted and given below. As our application requires low voltages, the motor is designed for these nominal low voltages and according to power rating current consumption is estimated.

Electrical Parameters

Rated Power (P_{rated})	25W
Power Factor (P.F or cosθ)	0.8
Nominal Voltage (V_L)	24V
Nominal Current (I)	0.75A – 1A
Connection Type	Star(Y) with internal neutral

Table 3-1: Electrical parameters of motor

Physical Parameters

Stator outer diameter (Do)	95mm
Stator inner diameter (Di)	55.5mm
Stator length (l_s)	22.5mm
Number of slots	24
Rotor outer diameter	55mm
Air gap	0.25mm

Table 3-2: Physical parameters of motor

After acquiring the physical and electrical parameters the design process is started. Flowing procedural steps are performed to complete the design process

i. Calculation of number of pole pairs

$$p = \frac{60 \times f}{n_S} = \frac{60 \times 50}{1500} = 2$$

p Number of pole pairs
f Nominal frequency (Hz)
n_S Rotational speed of magnetic field (°/min)

ii. Calculation of number of poles

$$P = p \times 2 = 2 \times 2 = 4$$

P Number of poles
p Number of pole pairs

iii. Calculation of number of slots per pole and phase

$$q = \frac{Z}{P \times m} = \frac{24}{4 \times 3} = 2$$

q Number of slots per pole and phase
Z Number of stator slots
P Number of poles
m Number of electric phases

iv. Calculation of pole step

$$\tau = \frac{Z}{2 \times p} = \frac{24}{2 \times 2} = 6$$

τ Pole step
Z Number of Stator slots

p Number of pole pairs

v. Calculation of pole step length

$$\tau_l = \frac{\pi \times D_i}{2 \times p} = \frac{3.14 \times 55.5}{2 \times 2} = 43.59 \cong 43.6mm$$

τ_l Pole step length (mm)
D_i Inner diameter of stator
p Number of pole pairs

vi. Calculation of pole surface area

$$Q_p = \tau_l \times l_s = 43.6 \times 22.5 = 1048.50mm^2 = 10.49cm^2$$

Q_p Pole surface area (cm^2)
τ_l Pole step length (mm)
l_s Length of stator (mm)

vii. Calculation of clean iron length (stator length)

$$l_z = k_z \times l_s = 0.94 \times 22.5 = 21.15mm$$

l_z Clean iron length (mm)
k_z Iron filling factor
l_s Length of stator (mm)

*Filling factor parameters

Height of Lammel (mm)	Type of isolation			No isolate
	Paper	Lacquer	Phosphate	
0.50	0.88	0.90	0.92	0.94
0.65	0.90	0.92	0.94	0.96

Table 3-3: Filling factor parameters

viii. Measurement of tooth length

$$h_z = 13.3mm$$

h_z Tooth length (mm)

ix. Measurement of tooth width

$$b_z = 3.70mm$$

b_z Tooth width (mm)

x. Calculation of height of yoke

$$h_j = \frac{1}{2}\left(D_o - D_i - (2 \times h_z)\right) = \frac{1}{2}(95 - 55.5 - (2 \times 13.3) = 6.45mm$$

h_j Height of yoke (mm)
D_o Outer diameter of stator (mm)
D_i Inner diameter of stator (mm)
h_z Tooth length (mm)

xi. Calculation of cross section area of yoke

$$Q_j = h_j \times l_z = 6.45 \times 21.15 = 136.42mm^2 = 1.36\ cm^2$$

Q_j Cross section area of yoke (cm^2)
h_j Height of yoke (mm)
l_z Clean iron length (mm)

xii. Calculation of cross section area of teeth of one pole

$$Q_z = \frac{Z \times b_z \times l_z}{2 \times p} = \frac{24 \times 3.70 \times 21.15}{2 \times 2} = 469.53mm^2 \cong 4.70cm^2$$

Q_z Cross section area of one tooth (cm^2)
Z Number of stator slots
b_z Tooth width (mm)
l_z Clean iron length (mm)
p Number of pole pairs

xiii. Induction in air gap

The value of magnetic field density or induction in air gap is selected from the given table below. It depends on number of poles. For the older motors with older cores value from column I is selected. Otherwise for new motors value from column II is chosen.

P	B_{zr} (T)	
	I	II
2	0.6 – 0.7	0.75 – 0.85
4	0.65 – 0.75	0.8 – 0.9
6	0.65 – 0.75	0.8 – 0.9
8	0.7 – 0.8	0.8 – 0.9
10	0.7 – 0.8	0.8 – 0.9

Table 3-4: Nominal magnetic flux

$$B_{zr} = 0.65 \text{ T}$$

B_{zr} Induction in air gap (T)

xiv. Calculation of induction in the teeth of the stator

$$B_z = B_{zr} \times \frac{Q_p}{Q_z} = 0.65 \times \frac{10.49}{4.70} = 1.45 \text{ T}$$

B_z Induction in teeth of stator (T)
B_{zr} Induction in air gap (T)
Q_p Surface area of pole (cm^2)
Q_z Cross section area of one tooth (cm^2)

xv. Calculation of induction in the stator yoke

$$B_j = \frac{B_{zr}}{\pi} \times \frac{Q_p}{Q_j} = \frac{0.65}{3.14} \times \frac{10.49}{1.36} = 1.60 \text{ T}$$

B_j Induction in stator yoke (T)
B_{zr} Induction in air gap (T)
Q_p Surface area of pole (cm^2)
Q_z Cross section area of yoke (cm^2)

The calculated value of magnetic field density or induction in stator yoke is compared with the value of induction in the teeth of the stator and checked if the fall in the range given in the table below.

P	B_j (T)	B_z (T)
2	1.6 – 2.1	1.0 – 1.6
4	1.5 – 2.0	1.2 – 1.7
6	1.5 – 1.9	1.3 – 1.7
8	1.5 – 1.9	1.3 – 1.7
10	1.5 – 1.9	1.3 – 1.7

Table 3-5: Comparison of magnetic flux between stator yoke vs stator teeth

xvi. Calculation of magnetic flux of one pair of poles

$$\phi = \frac{B_{zr} \times Q_p \times 1 \times 10^{-4}}{1.57} = \frac{0.65 \times 10.49 \times 1 \times 10^{-4}}{1.57} = 0.000435 \text{ Wb}$$

ϕ Magnetic flux of one pair of poles (Wb)
B_{zr} Induction in air gap (T)
Q_p Surface area of pole (cm^2)

xvii. Calculation of number of turns in the phase

$$w' = \frac{0.22 \times U_f \times a}{\phi \times f \times \xi} = \frac{0.22 \times 24 \times 1}{0.000435 \times 50 \times 0.958} = 253.40 \cong 254$$

w'	Number of turns in the coil
U_f	Phase voltage (V)
a	Number of parallel branches
ϕ	Magnetic flux of one pair of poles (Wb)
f	Nominal frequency (Hz)
ξ	Winding factor

xviii. Calculation Number of Turns in Slot

$$S'_u = \frac{6 \times w'}{Z} = \frac{6 \times 254}{24} = 63.5 \cong 64$$

S'_u	Number of turns in slot
w'	Number of turns in the coil

xix. Calculation of cross section of the wire

$$q'_v = \frac{Q_u \times f_u}{S'_u} = \frac{\times 0.34}{64} = mm^2$$

q'_v	Cross section of wire (mm^2)
Q_u	Cross sectional area of slot (mm^2)
f_u	Filling factor
S'_u	Number of turns in slot

xx. Calculation of thickness of wire

$$d'_Z = 2 \times \sqrt{\frac{q'_v}{\pi}} = 2 \times \sqrt{\frac{}{3.14}} = mm$$

d'_Z	Thickness (diameter) of wire (mm)
q'_v	Cross section of wire (mm^2)

xxi. Winding Diagram

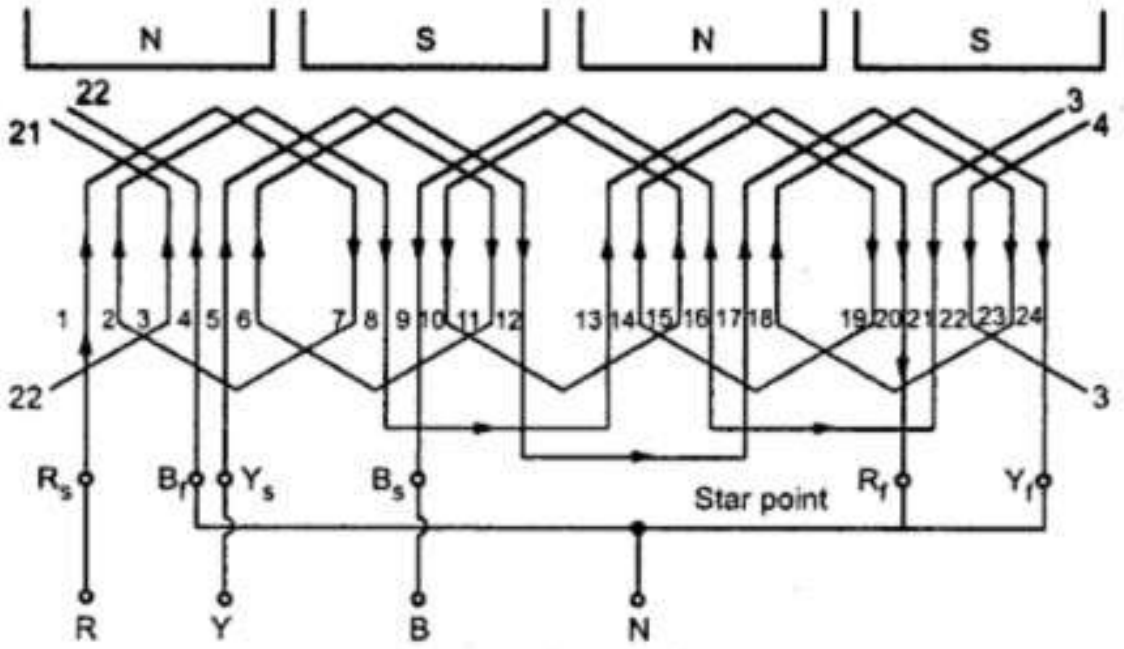

Figure 3-13: Winding diagram of 2 pole motor

3.6 Hardware Implementation

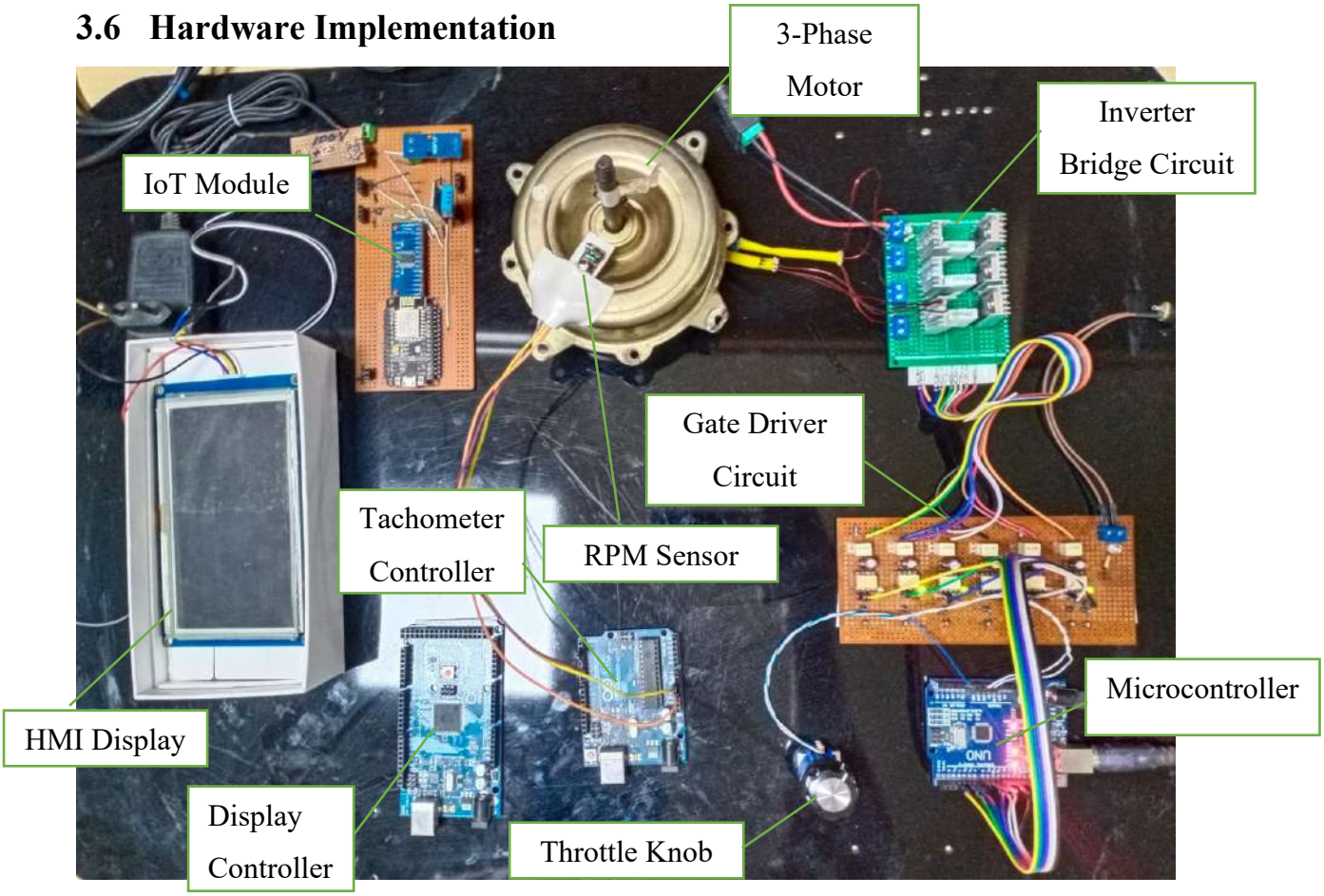

Figure 3-14: Hardware implementation – top view

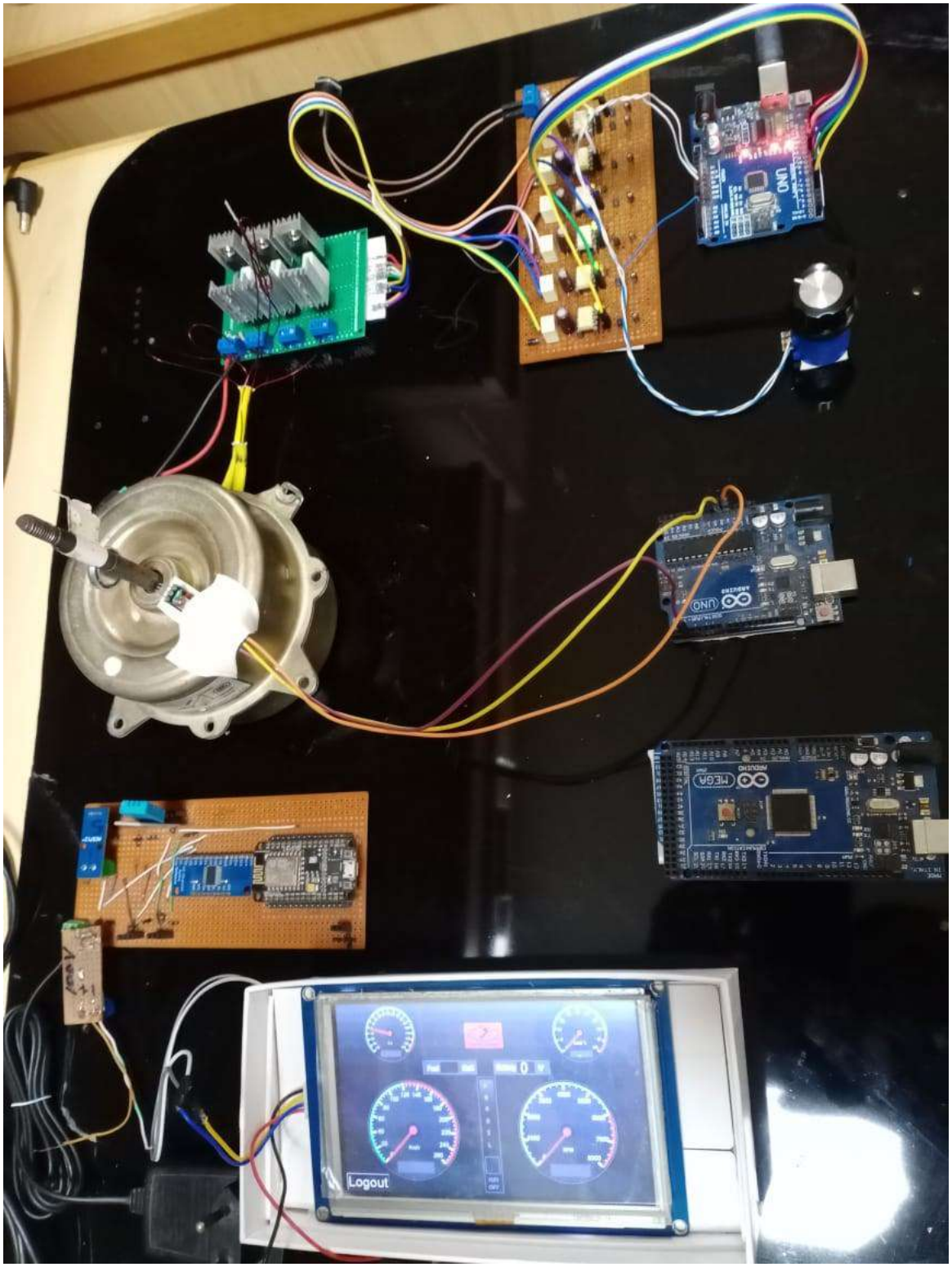

Figure 3-15: Hardware implementation – side view

3.7 Hardware Results

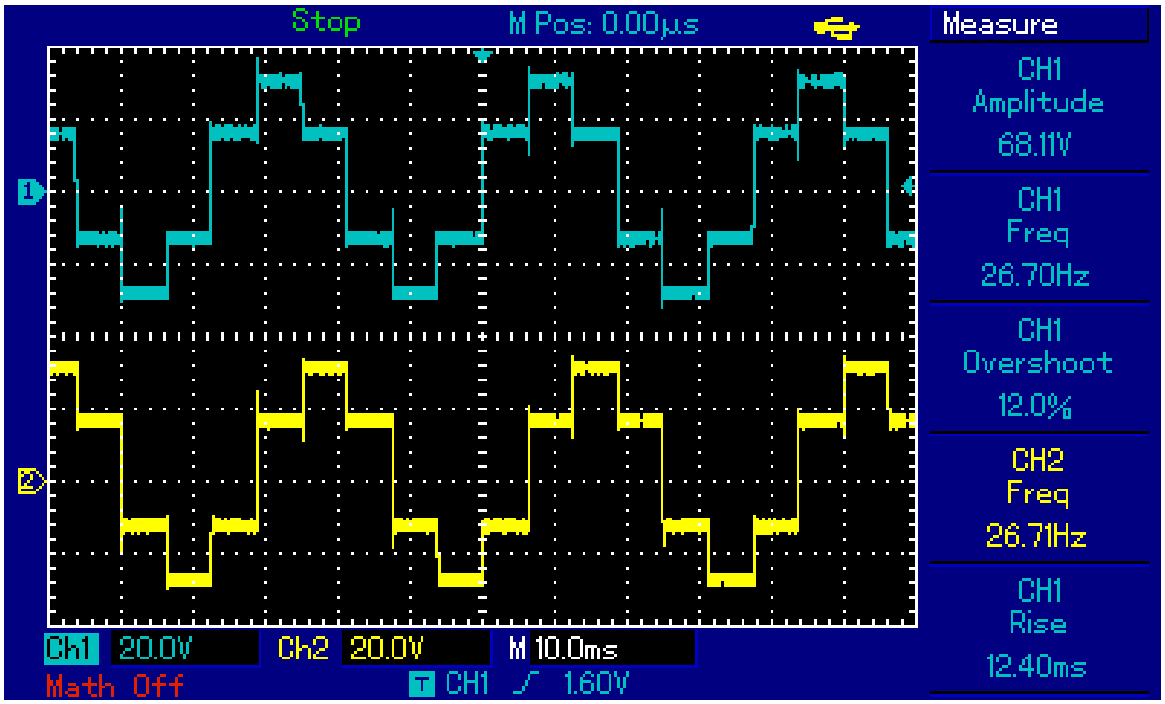

Figure 3-16: 120° conduction mode gate pulse

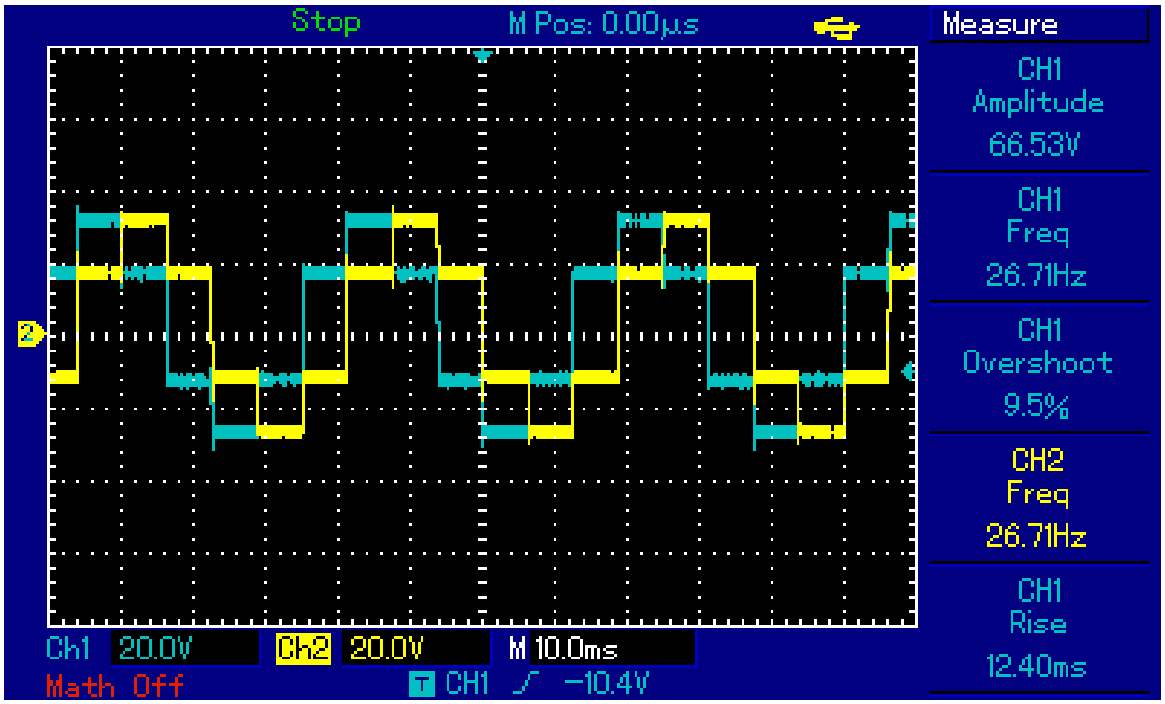

Figure 3-17: 120° conduction mode gate pulse with phase shift

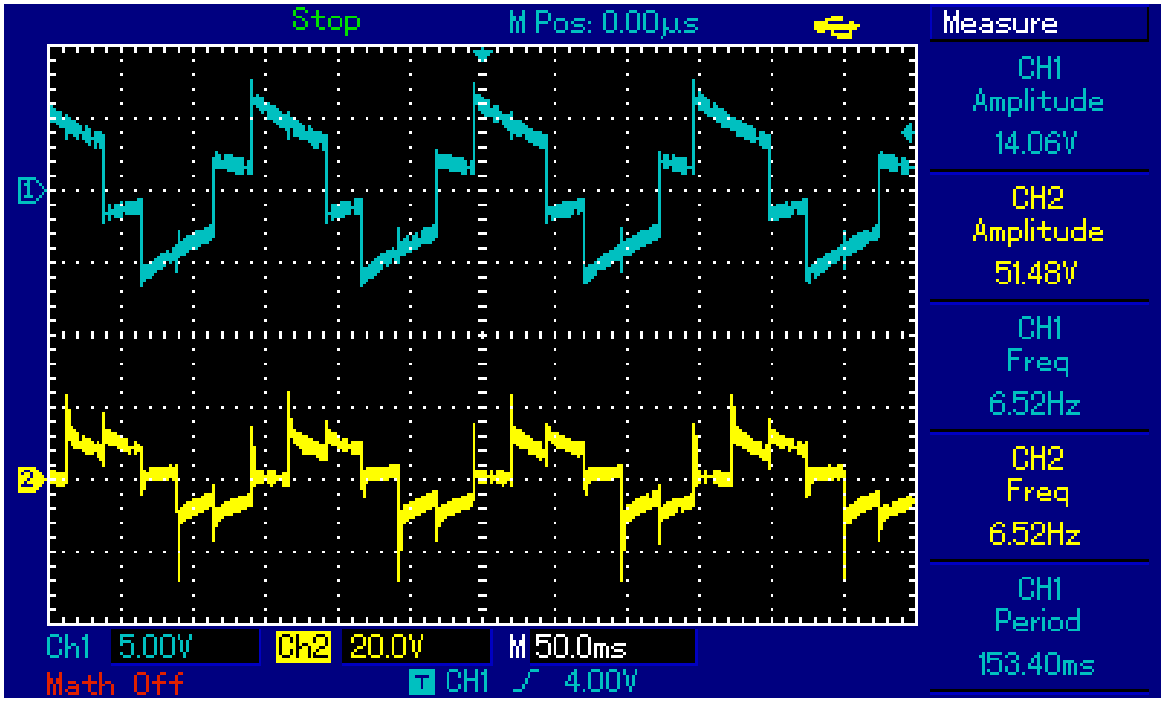

Figure 3-18: 120° conduction mode MOSFET output

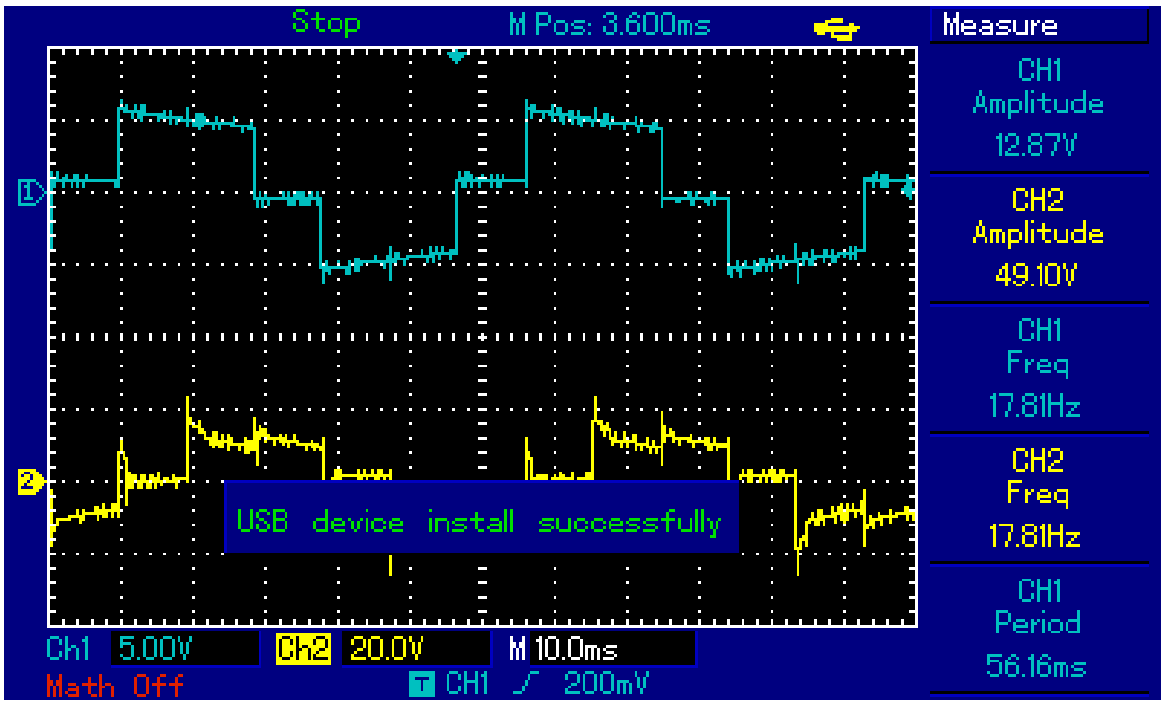

Figure 3-19: 180° conduction mode gate pulse and MOSFET output

Chapter 4

4 DATA ANALYSIS & DISCUSSION

4.1 Introduction

This chapter is about interpreting collected data in tabular form and then to visualize it in graphical trends. The collected data is then discussed to draw a meaningful conclusion.

The collected data is in relation to percentage throttle opening and various quantities as frequency, RPM, voltage, current and power consumption. These relation is also shown using graph to show how changing throttle position effects these quantities and what general trend can be predicted.

4.2 Collected Data

% Throttle	Frequency (Hz)	RPM
1	1	6
10	1.15	10
20	1.26	12
30	1.4	15
40	1.7	22
50	2	30
60	2.5	37
70	3.5	63
80	5.25	104
90	10.28	265
100	17.8	502

Table 4-1: Throttle vs Frequency & RPM

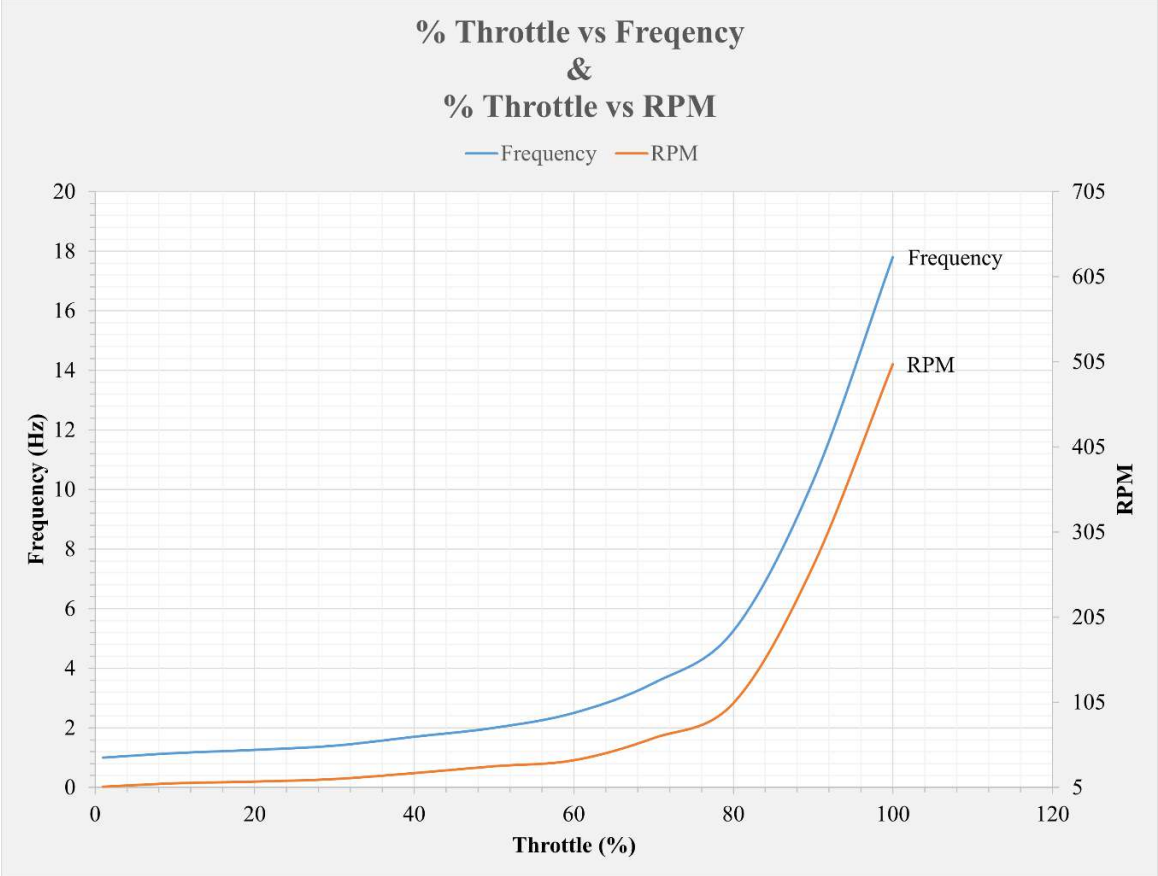

Figure 4-1: Graph between Throttle vs Frequency & RPM

% Throttle	Voltage (V)	Current (A)
1	15.2	0.28
10	15.3	0.38
20	15.3	0.46
30	15.5	0.63
40	15.4	0.71
50	15.5	0.85
60	15.3	0.89
70	15.1	0.91
80	15.1	0.95
90	15.2	0.92
100	15.3	0.89

Table 4-2: Throttle vs Voltage & Current

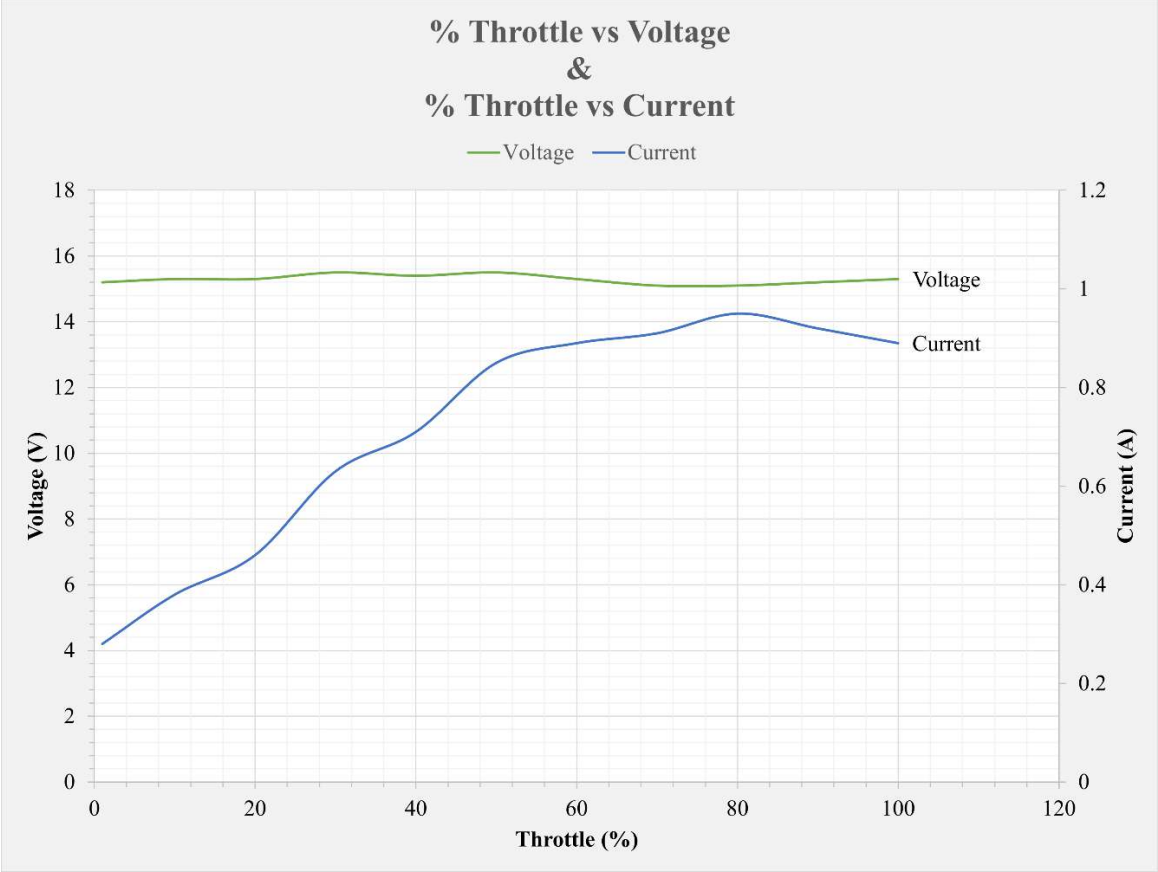

Figure 4-2: Graph between Throttle vs Voltage & Current

% Throttle	Power (W)
1	4.265
10	5.814
20	7.038
30	9.765
40	10.934
50	13.175
60	13.617
70	13.741
80	14.345
90	13.984
100	13.617

Table 4-3: Throttle vs Power

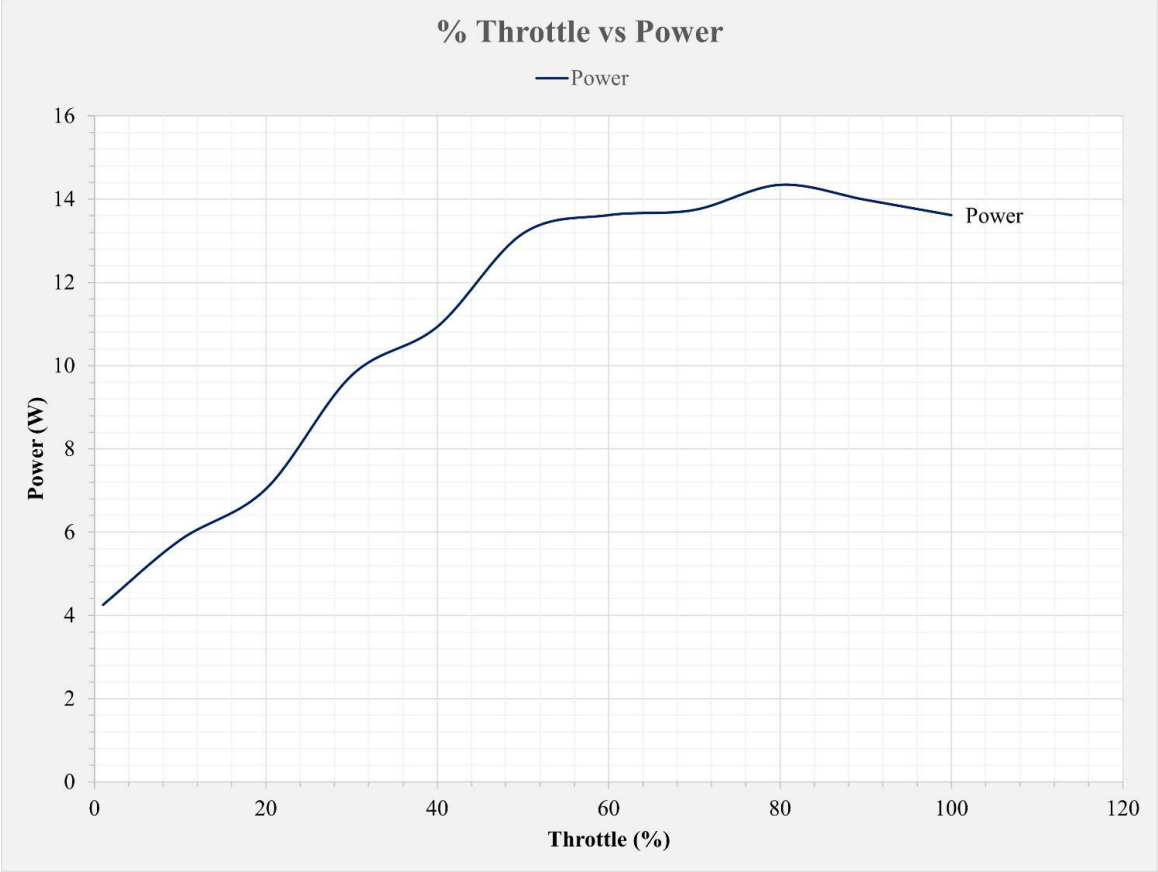

Figure 4-3: Graph between Throttle vs Power

4.3 Discussion

In the light of collected data, it is observed that with linear change in throttle position depicts a nonlinear change in frequency and RPM. As it can be seen that frequency and RPM changes slowly with change in throttle position but at last quarter position the frequency and RPM gets doubled. This is because the throttle position is mapped in microcontroller as 10-bit data so starting bits are small while last bits gets doubled from previous bit.

It is also observed that with change in throttle position the motor voltage somewhat remains constant with minimum fluctuations while the current increases with increase in throttle position. The increase in current is because with the increase in throttle position there is an increase in frequency, which dictates the magnetization and demagnetization of the core. Lastly the relation of throttle position and power consumption is observed. The power consumption is obtained from product of motor voltage and current supplied to motor. The power consumption follows the same trend as the current consumption as it is the product of two quantities.

Chapter 5

5 COST ANALYSIS & EXPENSES

5.1 Introduction

This chapter is about discussion of component cost and expenses of the project. Cost and expense analysis is very important part of any project as it gives insights about feasibility and realization of the project. It also compares the project with already available alternatives and enables us to decide whether we should choose this project. Also in view of production and marketing of a product cost analysis is also plays an important role

5.2 Bill of Quantities

Component	Price
Motor	5,000 /-
Arduino UNO	1,900 /-
Arduino MEGA	4,000 /-
MOSFETs	1,000 /-
TLP 250 Gate Drivers	1,500/-
Passive Components: Resistors, Capacitors, Diodes, jumper wires, Terminals, PCBs	4,000 /-
ESP 32	1,075 /-
NEXTION HMI	19,000 /-
Sensors: Current, Voltage, RPM etc.	2,500 /-
Battery	7,000 /-
TOTAL	46,975/-

Figure 5-1: Bill of quantities

Chapter 6

6 CONCLUSION

Today world population relies heavily on fossil fuels for their mobility needs. Fossil fuel is a scarce source and its limited quantity dictates its price. Moreover, the use of fossil fuels has an adverse on environment in form of global warming and climate change. This project and contents of this thesis is presented as an alternative to shift transport industry from fossil fuels to sustainable electric vehicles powered by renewable energy sources. This way the effect of burning of fossil fuels can be minimizes and hence shorten the carbon footprint.

The idea proposed in the thesis is to design an efficient electric vehicle drive system based on induction motors. Induction motors are powerful and has an advantage of having a simple and maintenance-free design with high efficiency and low cost. Induction motors to EVs is nothing new and many car manufactures has introduced there EV models with induction motors. To use induction motor in EVs its speed needs to controlled without using gear system so technique is used to change frequency of supply voltage to motor. This can be done with the help of an inverter. So the complete picture is that: battery gives DC supply to inverter which is converted to AC with variable frequency, supplied to motor, thus turning the wheels. Also with this drive system sensors and control system is designed with IoT (Internet of Things) functionality for best user experience.

6.1 Challenges Faced

While developing this project a number of challenges were faced and many hurdles have been overcome from the beginning till the end. The issues were faced during the phase of developing hardware system as well as during conceptualizing software algorithm. On a bright side, the challenges faced were not appeared as complicated, but they were the source of learning for all of us group members. Some of the challenges are listed below

- Simultaneous switching of upper and lower MOSFET in a phase (shoot-through fault).
- Damage to gate-drivers due to shoot-through fault.
- Dealing with high inrush current of the motor.
- Failing of MOSFETs due to much high current

The solution to above said challenges are listed below

- Use of dead time in software code for switch pulse. This can also be done using hardware circuit.
- Use of carefully calculated gate resistors to limit the current from gate driver to MOSFET gate.
- The inrush current is minimized by using soft start technique.
- MOSFETs are upgraded to high current ratings.

6.2 Other Applications

The project proposed in this thesis is not just limited to electric vehicle applications and can be used in many other aspects. Some of these applications are listed below.

- Three phases fixed frequency inverter.
- Three phase inverter for solar power applications.
- Use as STATic synchronous COMpensator (STATCOM).
- Induction motor speed control for domestic and industrial use.
- Soft starter for induction machines.
- Single phase to three phase inverter.
- HMI interface applications
- IoT applications

6.3 Suggestions for future work

The idea presented in this thesis is to build an electric drive system using power electronics. The principles and techniques used in the project can be improved and can be changed for more personalized applications. Below are some aspects which are open to further modification.

- Implementation of Space Vector Pulse width modulation (SVPWM).
- Implementation of multi-level inverter.
- Bidirectional system with battery charging system.
- Scalability of the system to high voltage and high power.
- Upgrading the battery packs.

Chapter 7

7 REFERENCES

[1] Martin Weiss, Peter Dekker, Alberto Moro, Harald Scholz, Martin K. Patel, On the electrification of road transportation – A review of the environmental, economic, and social performance of electric two-wheelers, Transportation Research Part D: Transport and Environment, Volume 41, 2015, Pages 348-366,

[2] T. Ilahi, T. Zahid, M. Zahid, M. Iqbal, A. Sindhila, and Q. Tahir, 'Design Parameter and Simulation Analysis of Electric Bike Using Bi-Directional Power Converter', in 2020 International Conference on Electrical, Communication, and Computer Engineering

[3] T. Ilahi et al., 'Design and Performance Analysis of Ultra-Wide Bandgap Power Devices-Based EV Fast Charger Using Bi-Directional Power Converters', IEEE Access, vol. 11, pp. 25285–25297, 2023, doi: 10.1109/ACCESS.2023.3255780.

[4] Bilal Akin and Nishant Garg," Scalar (V/f) Control of 3-Phase Induction Motors", Texas Instruments, SPRABQ8–July 2013

[5] N. Roshan, T. Ilahi, T. Zahid, M. Zahid, M. Ali, and Q. Awais, "Design of HMI Based Digital Electric Bike Using DC/AC Power Converter with Regenerative Feature," Pakistan J. Eng. Technol., vol. 4, no. 3, pp. 1–7, 2021, doi: 10.51846/vol4iss3pp1-7.

[6] M.P. Kazmier kowski, "Control strategies for PWM rectifier/inverter-fed induction motors Inst. of Control & Ind. Electron, Volume: 08 , Issue: 10, Year: 2011

[7] A. Mohammad, M. A. Abedin, and M. Z. R. Khan, "Microcontroller Based Control System for Electric Vehicle," International Conference on Informatics, Electronics & Vision (ICIEV 2016), pp. 1-4, May 2016.

[8] L. Alberti and D. Troncon, "Design of Electric Motors and Power Drive Systems According to Efficiency Standards," in IEEE Transactions on Industrial Electronics, vol. 68, no. 10, pp. 9287-9296, Oct. 2021, doi: 10.1109/TIE.2020.3020028.

[9] Itani K, De Bernardinis A. Review on New-Generation Batteries Technologies: Trends and Future Directions. Energies. 2023; 16(22):7530. https://doi.org/10.3390/en16227530

[10] X. Y. Xu, "Developement of transmission technology for energy-saving vehicles and new energy resource vehicle," Journal of Automotive Safety and Energy., vol. 8, no. 4, pp. 323–332, 2017.

[11] J. H. Liu, "Matching design of powertrain parameters of pure electric vehicle. Auto," Manufacturing Engineering, vol. 3, p. 57-58+61, 2018.